AIMS Mathematics, 11(1): 1117–1144.
DOI: 10.3934/math.2026048
Received: 10 October 2025
Revised: 27 November 2025
Accepted: 02 December 2025
Published: 15 January 2026

https://www.aimspress.com/journal/Math

Research article

Impact of double Allee effect on the dynamics and stability of a predator-prey model

Asifa Tassaddiq[1], Rizwan Ahmed[2], Jawad Khan[3,*] and Youngmoon Lee[4,5,*]

[1] Department of Computer Science, College of Computer and Information Sciences, Majmaah University, Al Majmaah 11952, Saudi Arabia
[2] Department of Mathematics, Air University Multan Campus, Multan 60001, Pakistan
[3] School of Computing, Gachon University, Seongnam 13120, Republic of Korea
[4] Department of Robotics, Hanyang University, Ansan 15588, Republic of Korea
[5] Department of Applied AI, Hanyang University, Ansan 15588, Republic of Korea

* **Correspondence:** Email: jkhanbk1@gachon.ac.kr; youngmoonlee@hanyang.ac.kr.

Abstract: In this paper, we investigated the complex dynamics of a discrete-time predator-prey model incorporating a double Allee effect in the prey population. We investigated the existence and stability of biologically meaningful fixed points, including extinction, prey-only, and coexistence equilibria. Through analytical and numerical bifurcation analysis, we demonstrated that the model underwent a Neimark-Sacker bifurcation as key parameters varied, leading to quasi-periodic oscillations that characterized realistic population cycles. Our results revealed that stronger Allee effects tend to destabilize the model, increasing extinction risks and promoting oscillatory dynamics, while higher predator mortality rates and saturation in predation response enhance stability. A comparative analysis with models lacking the Allee effect highlights its critical role in delaying equilibrium convergence and inducing instability at low population densities. These findings provide important insights for ecological conservation, particularly for species vulnerable to population depletion, and contribute to the theoretical understanding of predator-prey models with density-dependent growth constraints.

Keywords: predator-prey model; Allee effect; stability; bifurcation
Mathematics Subject Classification: 39A28, 39A30

1. Introduction

Predator-prey interactions are essential elements of ecological models, influencing the population dynamics of species across many environments. The conventional Lotka-Volterra model, first

developed by Lotka [1] and Volterra [2], offers a fundamental framework for examining predator-prey interactions. This model, while fundamental in theoretical ecology, inadequately represents the complex characteristics of actual ecological systems due to its oversimplified structure. Researchers have discovered many elements that substantially alter these interactions, including functional responses [3], harvesting [4], cannibalism [5], fear-induced behaviors [6, 7], prey refuge [8], and the Allee effect [9–11]. To more effectively include these ecological intricacies, researchers have devised several extensions of the original framework.

The Allee effect, first identified by Allee [12], is a biological phenomenon whereby populations experience reduced per capita growth rates at low densities. This reduction may be ascribed to challenges in mate acquisition, diminished efficacy in group defense, or inadequacies in collective foraging. Consequently, populations may encounter critical density limits under which extinction becomes increasingly likely. Usually, the Allee effect is classified as either strong or weak. With a strong Allee effect, populations below a certain threshold cannot survive and go toward extinction. On the other hand, a weak Allee effect just reduces population growth at low densities without necessarily driving the species toward extinction. In addition to theoretical work, Allee effects are well documented in real ecological systems. Strong Allee effects appear in species such as Atlantic cod, where individuals have difficulty finding mates and feeding efficiently at very low densities, leading to several observed stock collapses. Cooperative mammals such as African wild dogs also show a strong Allee effect, when pack size falls below a critical level, group hunting becomes ineffective and the population cannot sustain itself. Weak Allee effects are also common in nature. For example, many insects and marine invertebrates show reduced reproductive success when population density is low, even though they can persist above very small population sizes. These cases show that low-density difficulties, whether strong or weak, are widespread in nature and can play an important role in population stability and extinction risk, underscoring the importance of incorporating Allee effects into predator-prey models. The Allee effect on prey populations may significantly affect predator-prey dynamics, leading to bistability, numerous stable states, and increased extinction risk for predators and prey.

Several studies have shown the critical impact of the Allee effect on the dynamics of predator-prey models. Shang and Qiao [13] examined a model in which the prey exhibits a strong Allee effect, revealing that it results in heteroclinic bifurcations and a reduction in the number of limit cycles, hence influencing the model's overall stability. Kumbakar et al. [14] examined the effects of a strong Allee effect on prey populations, revealing that it may lead to bistability and tristability, underlining the importance of initial population levels in shaping long-term behavior. Zhang and Wang [15] investigated a discrete-time predator-prey model incorporating a weak Allee effect on predators, demonstrating its influence on codimension-one bifurcations and the appearance of chaotic dynamics, which exhibits significant sensitivity to parameter values and initial conditions. Furthermore, Dong et al. [16] studied a delayed population model, including a weak Allee effect, and concluded that the delay might enhance stability, transitioning the model from unstable to stable regimes. Furthermore, Zeng and Yu [17] conducted a comprehensive study on multiple predator-prey models and concluded that incorporating the Allee effect significantly increases dynamical richness by inducing bifurcations such as Hopf and Bogdanov-Takens, which are not observed in models lacking this effect. Liu et al. [18] investigated how the Allee effect on prey impacts a Leslie-Gower model with hunting cooperation. It was demonstrated that increasing the intensity of the Allee could destabilize

coexistence and cause various bifurcations, such as saddle-node, Hopf, and Bogdanov-Takens. Their work indicates that for high-intensity Allee effects, the predator-prey model is more sensitive to species extinction. Various dynamic outcomes, such as multistability and high-codimension bifurcation resulting from the Allee mechanism, were demonstrated by Chen et al. [19] in the context of a Leslie-Gower predator-prey model with strong Allee effects. Their work emphasized how the strength of an Allee effect, in addition to the availability of prey refuge, is very important for the dynamics of species coexistence.

We start by examining the predator-prey model proposed in [20], which includes a strong Allee effect for the prey species and a Holling type II functional response for the predator:

$$\begin{cases} \frac{dX}{dT} = rX(1-\frac{X}{k})(X-A) - bXY, \\ \frac{dY}{dT} = Y(\frac{\lambda bX}{1+bhX} - d), \end{cases} \tag{1.1}$$

where $X(T)$ and $Y(T)$ denote the densities of the prey and predator populations at time T, respectively. The parameter r represents the intrinsic growth rate of the prey, while k is its carrying capacity. A denotes the Allee threshold, indicating the critical density below which the prey population may decline. b is the predation rate, λ is the conversion efficiency of prey into predator biomass, h is the handling time of the predator, and d represents the predator's natural mortality rate. The study in [20] showed that a strong Allee effect can destabilize the model, leading to the emergence of limit cycle oscillations and raising the risk of prey extinction. Their investigation revealed various forms of bifurcations, including transcritical and Hopf bifurcations, underlining the considerable significance of the Allee effect on population dynamics.

While most of the predator-prey models use a single Allee effect, relatively fewer researchers have dealt with the incorporation of double Allee effects. The double Allee mechanism appears when there are two different biological processes that independently restrain the population growth at low densities. Such dual limitations may arise from ecological factors such as impaired mating opportunities, poor reproductive success, or weakened cooperative defense against predators. The inclusion of double Allee effect thus gives a more realistic representation of the issues faced by small populations. We note that exploring the effects of this combined mechanism on predator-prey dynamics is essential to capture the richer and more involved dynamics in nature and represents the novelty in extending the model (1.1), including double Allee effect.

Numerous researchers have investigated predator-prey models, including double Allee effects, uncovering a variety of intricate dynamics. Tiwari and Raw [21] examined a Leslie-Gower model, including double Allee effects and predator interference. Their analysis revealed multistability, Hopf bifurcations, and spatial configurations, including circular and rhombus-shaped patterns arising from Turing instability. Wang et al. [22] investigated a reaction-diffusion predator-prey model that integrates the double Allee effect. They demonstrated the formation of spatial patterns, including spots and stripes, and validated their analytical results using numerical simulations. Jiao and Chen [23] examined a delayed predator-prey model, including the double Allee effect, demonstrating the interplay between delay and Allee effects that results in Bogdanov-Takens bifurcation and intricate dynamic behaviors. Mandal et al. [24] incorporated prey refuge and double Allee effects, revealing codimension-one and two bifurcations, bi- and tri-stability, and showing that double Allee effect significantly increases model complexity. Pal and Saha [25] conducted a detailed bifurcation analysis of a ratio-dependent model with the double Allee effect in prey, identifying bi-stability, separatrix curves, and multiple bifurcation

phenomena, including Bogdanov-Takens, Hopf, and homoclinic bifurcations, emphasizing sensitivity to initial conditions and ecological implications. Wang and Yang [26] illustrated that integrating a double Allee effect in the prey population considerably affects the stability and coexistence of species, containing oscillatory dynamics often via Hopf bifurcation. Mondal et al. [27] investigated how the double Allee effect alters both continuous and discrete predator-prey systems, revealing that Allee intensity can enhance or destabilize system stability depending on its strength. They demonstrated that weak Allee effects increase extinction risk, while strong Allee effects promote stability and can lead to multistability and complex bifurcation behaviors.

Motivated by the above studies, we modify model (1.1) by incorporating a double Allee effect in the prey population, leading to the following model:

$$\begin{cases} \frac{dX}{dT} = rX(1-\frac{X}{k})(\frac{X-m}{X+l}) - bXY, \\ \frac{dY}{dT} = Y(\frac{\lambda bX}{1+bhX} - d), \end{cases} \tag{1.2}$$

where condition $l < k$ is imposed for biological plausibility, and m lies within the interval $(-k, k)$. The first Allee effect is represented by the term $X - m$, which models reduced reproductive success when the prey population falls below the threshold m. The second Allee effect is introduced through the factor $\frac{X}{X+l}$, which increases monotonically with prey density. Biologically, this term captures additional density-dependent limitations arising at low population sizes. When X is small relative to l, the ratio $\frac{X}{X+l}$ becomes significantly less than one, reducing the effective growth rate of the prey. This reflects situations where the population experiences constraints such as limited availability of fertile individuals, impaired cooperative defense, or difficulties in group foraging, even when the classical Allee threshold is not explicitly crossed. The functional form approaches one as X increases, meaning these subsidiary density-dependent inhibitions diminish when population densities are high. Therefore, the system includes two separate biological mechanisms that each reduce population growth at low densities, enhancing the ecological realism of the model.

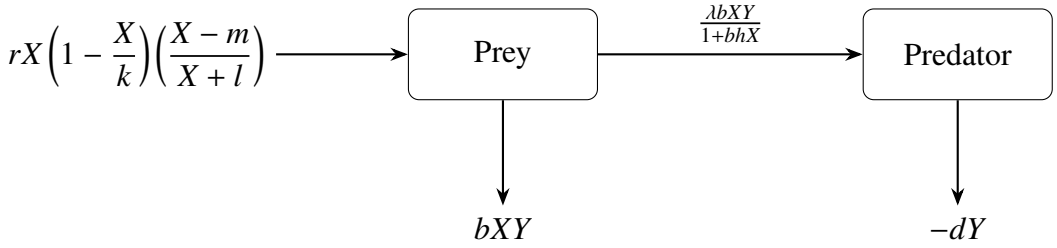

Figure 1. Flowchart of the predator-prey model (1.2).

To reduce the number of parameters, we introduce the following transformations:

$$x = \frac{X}{k},\ y = \frac{bY}{r},\ t = rT.$$

Then, we obtain the following non-dimensional form of (1.2):

$$\begin{cases} \frac{dx}{dt} = x(1-x)(\frac{x-\alpha}{x+\beta}) - xy, \\ \frac{dy}{dt} = y(\frac{\gamma x}{1+\eta x} - \sigma), \end{cases} \tag{1.3}$$

where $\alpha = \frac{m}{k}, \beta = \frac{l}{k}, \gamma = \frac{kb\lambda}{r}, \eta = bhk$, and $\sigma = \frac{d}{r}$. One can see that β, γ, η, and σ are positive constants and $\alpha \in (-1, 1)$.

In contrast, discrete-time models are particularly suited to describe populations with nonoverlapping generations, distinct reproductive cycles, and seasonal breeding patterns. Typical examples are insects such as mayflies that have short, synchronized life cycles, or anadromous fish such as Pacific salmon whose life history is marked by distinct generational cycles. Additionally, discrete-time systems are renowned for their ability to produce complex dynamics like period-doubling (PD) bifurcations, Neimark-Sacker (NS) bifurcations, and chaotic behavior that are rarely observed in continuous systems [28–30]. Significantly, in contrast to two-dimensional continuous systems, the discrete maps can also be chaotic in one dimension; for instance, the logistic map, which implies a richer spectrum of possible dynamics in populations. Thus, the choice of discretization method is a delicate task because it sometimes drastically affects whether or not the discrete model inherits the qualitative dynamics from the original continuous model. Though the forward Euler method is a commonly used and simple discretization technique [31, 32], it may introduce inconsistencies into the model, such as negative population values that do not make biological sense. For this reason, we make use of the piecewise constant argument method [33–35] ensures non-negative solutions while preserving much of the dynamical behavior of the original model.

By applying piecewise constant arguments to address non-linear differential equations and accounting for consistent time intervals that represent the mean growth rates of both species, (1.3) can be reformulated as

$$\begin{cases} \frac{1}{x(t)}\frac{dx}{dt} = (1 - x[t])(\frac{x[t]-\alpha}{x[t]+\beta}) - y[t], \\ \frac{1}{y(t)}\frac{dy}{dt} = \frac{\gamma x[t]}{1+\eta x[t]} - \sigma. \end{cases} \tag{1.4}$$

Here, $[t]$ denotes the integer part of t, where $0 < t < \infty$. Moreover, by integrating (1.4) over the interval $[n, n + 1)$ for $n = 0, 1, 2, \ldots$, we obtain

$$\begin{cases} x_t = x_n e^{(\frac{(1-x_n)(x_n-\alpha)}{x_n+\beta} - y_n)(t-n)}, \\ y_t = y_n e^{(\frac{\gamma x_n}{1+\eta x_n} - \sigma)(t-n)}. \end{cases} \tag{1.5}$$

By letting $t \to n + 1$, we obtain

$$\begin{cases} x_{n+1} = x_n e^{\frac{(1-x_n)(x_n-\alpha)}{x_n+\beta} - y_n}, \\ y_{n+1} = y_n e^{\frac{\gamma x_n}{1+\eta x_n} - \sigma}. \end{cases} \tag{1.6}$$

Through the integration of a dual Allee effect and implementation of a discrete-time approach, in this investigation, we advance the comprehension of predator-prey interactions in ecologically realistic scenarios. Moreover, this study furthers our theoretical understanding of density-dependent populations while offering practical applications for species conservation and ecosystem management through its characterization of critical population thresholds.

The organization of the paper is as follows: In Section 2, we investigate the existence and topological classification of the equilibrium points, while in Section 3, we explore the local bifurcation phenomena occurring at the positive equilibrium. In Section 4, we present numerical simulations that support and illustrate the analytical results. We conclude with a summary of the key findings in Section 5.

2. Existence and stability of fixed points

In this section, we consider fixed points of the model and investigate their local stability properties. A fixed point is an ecological equilibrium where both species' population sizes become fixed from generation to generation. Stability assessment is biologically crucial because it provides insight into whether small environmental or demographic perturbations are self-correcting, that is, return the system to the equilibrium, or magnify and drive the populations from the steady state. Local dynamics around these states are characterized by the Jacobian matrix and its eigenvalues at each equilibrium. Such information is key to understanding persistence, coexistence, extinction risks, and other long-term ecological outcomes predicted by the model.

2.1. Analysis of fixed points' existence

The fixed points (x, y) of (1.6) can be found by solving the following system:

$$\begin{cases} x = xe^{(1-x)(\frac{x-\alpha}{x+\beta})-y}, \\ y = ye^{\frac{\gamma x}{1+\eta x}-\sigma}. \end{cases} \tag{2.1}$$

Solving the above equations yields four fixed points:

$$E_0 = (0, 0),\ E_1 = (1, 0),\ E_2 = (\alpha, 0),$$

$$E_3 = \Big(\frac{\sigma}{\gamma - \eta\sigma}, -\frac{(\gamma - (\eta + 1)\sigma)(\alpha\gamma - \sigma(\alpha\eta + 1))}{(\gamma - \eta\sigma)(\beta(\gamma - \eta\sigma) + \sigma)}\Big).$$

Each fixed point has a meaningful biological interpretation:

- $E_0 = (0, 0)$: This represents the extinction equilibrium, indicating the complete demise of both species. It signifies an environmentally degraded situation, often unfavorable or occurring under severe circumstances.
- $E_1 = (1, 0)$: In this condition, species x exists independently with a population of $x = 1$, but species y is nonexistent. This equilibrium indicates that species x may achieve stability by self-limiting development, irrespective of species y.
- $E_2 = (\alpha, 0)$: In this scenario, species x endures at a diminished level $x = \alpha$ in the absence of species y. The fixed point occurs just when $\alpha > 0$, indicating that the parameter α influences the solitary survival of species x.
- $E_3 = (\bar{x}, \bar{y})$: This is an interior equilibrium representing the coexistence of both species. For E_3 to be biologically meaningful (i.e., $\bar{x} > 0$ and $\bar{y} > 0$), the following conditions must be satisfied:

$$\gamma > \sigma(1 + \eta),\ \alpha\gamma < \sigma(1 + \alpha\eta).$$

These requirements guarantee that species y derives enough advantage from its interaction with species x to offset its natural mortality rate σ, while species x remains unaffected by excessive suppression from species y.

As a result, the model demonstrates many ecological outcomes, including extinction, solitary species survival, and mutual cohabitation. Recognizing these fixed points is essential for

comprehending the model's long-term dynamics, hence facilitating further stability and bifurcation investigations.

2.2. Stability analysis of fixed points

To analyze the local dynamics near each equilibrium, we compute the Jacobian matrix of model (1.6) at any fixed point (x, y):

$$J(x,y) = \begin{bmatrix} \frac{e^{-\frac{(-1+x)x}{A+x}-by}(A^2+A(3-2x)x-(-1+x)x^2)}{(A+x)^2} & -be^{-\frac{(-1+x)x}{A+x}-by}x \\ ce^{m+cx-y}y & -e^{m+cx-y}(-1+y) \end{bmatrix}. \tag{2.2}$$

Let θ_1 and θ_2 be the eigenvalues of $J(x, y)$. The type of each fixed point is then characterized based on the modulus of these eigenvalues:

Definition 2.1. *A fixed point* (x, y) *of system* (1.6) *is characterized as follows:*

(1) It is called a sink if both eigenvalues satisfy $|\theta_1|< 1$ *and* $|\theta_2|< 1$.
(2) It is a source if $|\theta_1|> 1$ *and* $|\theta_2|> 1$.
(3) It is classified as a saddle when one eigenvalue lies inside and the other outside the unit circle, i.e., $\max\{|\theta_1|, |\theta_2|\} > 1$ *and* $\min\{|\theta_1|, |\theta_2|\} < 1$.
(4) The point is said to be non-hyperbolic if at least one eigenvalue satisfies $|\theta_i|= 1$ *for* $i = 1, 2$.

When the eigenvalues take a complicated form, direct use of this definition is not straightforward. Therefore, the next result provides an effective approach for analyzing the stability of the fixed point.

Lemma 2.2. *[36] Consider the quadratic polynomial* $\Delta(\theta) = \theta^2 + K_1\theta + K_0$. *Assume that* $\Delta(1) > 0$. *Let* θ_1 *and* θ_2 *be the roots of* $\Delta(\theta) = 0$. *Then the following statements hold:*

(1) Both eigenvalues satisfy $|\theta_1|< 1$ *and* $|\theta_2|< 1$ *if* $\Delta(-1) > 0$ *and* $K_0 < 1$.
(2) One eigenvalue lies inside and the other outside the unit circle, i.e., $|\theta_1|< 1 < |\theta_2|$ *(or vice versa), if* $\Delta(-1) < 0$.
(3) Both eigenvalues satisfy $|\theta_1|> 1$ *and* $|\theta_2|> 1$ *if* $\Delta(-1) > 0$ *and* $K_0 > 1$.
(4) The roots θ_1 *and* θ_2 *are complex with* $|\theta_{1,2}|= 1$ *when* $K_1^2 - 4K_0 < 0$ *and* $K_0 = 1$.

Proposition 2.3. *The trivial fixed point* E_0 *is*

(1) a sink if $0 < \alpha < 1$,
(2) never a source,
(3) a saddle if $-1 < \alpha < 0$,
(4) non-hyperbolic if $\alpha = 0$.

Proof. We obtain

$$J(E_0) = \begin{bmatrix} e^{-\frac{\alpha}{\beta}} & 0 \\ 0 & e^{-\sigma} \end{bmatrix}. \tag{2.3}$$

The eigenvalues of $J(E_0)$ are $\theta_1 = e^{-\frac{\alpha}{\beta}}$ and $\theta_2 = e^{-\sigma}$. Clearly, $|\theta_2|< 1$. Moreover,

$$\left|e^{-\frac{\alpha}{\beta}}\right| \begin{cases} < 1, & 0 < \alpha < 1, \\ = 1, & \alpha = 0, \\ > 1, & -1 < \alpha < 0. \end{cases} \tag{2.4}$$

Proposition 2.4. *The fixed point E_1 is*

(1) a sink if $0 < \gamma < \sigma(1+\eta)$,
(2) never a source,
(3) a saddle if $\gamma > \sigma(1+\eta)$,
(4) non-hyperbolic if $\gamma = \sigma(1+\eta)$.

Proof. We obtain

$$J(E_1) = \begin{bmatrix} \frac{\alpha+\beta}{1+\beta} & -1 \\ 0 & e^{\frac{\gamma}{1+\eta}-\sigma} \end{bmatrix}. \tag{2.5}$$

The eigenvalues of $J(E_1)$ are $\theta_1 = \frac{\alpha+\beta}{1+\beta}$ and $\theta_2 = e^{\frac{\gamma}{1+\eta}-\sigma}$. Clearly, $|\theta_1| < 1$. Moreover,

$$\left|e^{\frac{\gamma}{1+\eta}-\sigma}\right| \begin{cases} < 1, \ 0 < \gamma < \sigma(1+\eta), \\ = 1, \ \gamma = \sigma(1+\eta), \\ > 1, \ \gamma > \sigma(1+\eta). \end{cases} \tag{2.6}$$

Proposition 2.5. *The fixed point E_2 is*

(1) never a sink,
(2) a source if $\gamma > \frac{\sigma(1+\alpha\eta)}{\alpha}$,
(3) a saddle if $0 < \gamma < \frac{\sigma(1+\alpha\eta)}{\alpha}$,
(4) non-hyperbolic if $\gamma = \frac{\sigma(1+\alpha\eta)}{\alpha}$.

Proof. We obtain

$$J(E_2) = \begin{bmatrix} 1 + \frac{\alpha(1-\alpha)}{\alpha+\beta} & -\alpha \\ 0 & e^{\frac{\alpha\gamma}{1+\alpha\eta}-\sigma} \end{bmatrix}. \tag{2.7}$$

The eigenvalues of $J(E_2)$ are $\theta_1 = 1 + \frac{\alpha(1-\alpha)}{\alpha+\beta}$ and $\theta_2 = e^{\frac{\alpha\gamma}{1+\alpha\eta}-\sigma}$. Since $0 < \alpha < 1$, therefore, $|\theta_1| > 1$. Moreover, we obtain

$$\left|e^{\frac{\alpha\gamma}{1+\alpha\eta}-\sigma}\right| \begin{cases} < 1, \ 0 < \gamma < \frac{\sigma(1+\alpha\eta)}{\alpha}, \\ = 1, \ \gamma = \frac{\sigma(1+\alpha\eta)}{\alpha}, \\ > 1, \ \gamma > \frac{\sigma(1+\alpha\eta)}{\alpha}. \end{cases} \tag{2.8}$$

Next, we investigate the local stability of the positive fixed point $(\bar{x}, \bar{y}) = E_3$ of model (1.6). The Jacobian matrix at positive equilibrium $(\bar{x}, \bar{y})$ is given by

$$J(\bar{x}, \bar{y}) = \begin{bmatrix} w_{11} & -\bar{x} \\ \frac{\gamma\bar{y}}{(1+\bar{x}\eta)^2} & 1 \end{bmatrix}, \tag{2.9}$$

where $w_{11} = \frac{-\bar{x}^3+\bar{x}^2(1-2\beta)+\beta^2+\bar{x}(\alpha+3\beta+\alpha\beta)}{(\bar{x}+\beta)^2}$. The corresponding characteristic polynomial is

$$\Delta(\theta) = \theta^2 + (-1 - w_{11})\theta + w_{11} + \frac{\bar{x}\bar{y}\gamma}{(1+\bar{x}\eta)^2}.$$

It can be obtained through calculations that

$$\Delta(0) = w_{11} + \frac{\bar{x}\bar{y}\gamma}{(1+\bar{x}\eta)^2}, \ \Delta(-1) = 2 + 2w_{11} + \frac{\bar{x}\bar{y}\gamma}{(1+\bar{x}\eta)^2}, \ \Delta(1) = \frac{\bar{x}\bar{y}\gamma}{(1+\bar{x}\eta)^2}.$$

Thus, $\Delta(1) > 0$. By choosing $\Delta(-1) > 0$, we get

$$2 + 2w_{11} + \frac{\bar{x}\bar{y}\gamma}{(1 + \bar{x}\eta)^2} > 0,$$

$$\gamma > -\frac{2(1 + w_{11})(1 + \bar{x}\eta)^2}{\bar{x}\bar{y}}.$$

Similarly, $\Delta(-1) < 0$ is equivalent to $\gamma < -\frac{2(1+w_{11})(1+\bar{x}\eta)^2}{\bar{x}\bar{y}}$. Next, setting $\Delta(0) < 1$ implies that

$$w_{11} + \frac{\bar{x}\bar{y}\gamma}{(1 + \bar{x}\eta)^2} < 1,$$

$$\gamma < \frac{(1 - w_{11})(1 + \bar{x}\eta)^2}{\bar{x}\bar{y}}.$$

Similarly, $\Delta(0) > 1$ is equivalent to $\gamma > \frac{(1-w_{11})(1+\bar{x}\eta)^2}{\bar{x}\bar{y}}$ and $\Delta(0) = 1$ is equivalent to $\gamma = \frac{(1-w_{11})(1+\bar{x}\eta)^2}{\bar{x}\bar{y}}$. As a result, we obtain the following result:

Theorem 2.6. *The positive fixed point $E_3 = (\bar{x}, \bar{y})$ of the model* (1.6) *is*

(1) a sink if $-\frac{2(1+w_{11})(1+\bar{x}\eta)^2}{\bar{x}\bar{y}} < \gamma < \frac{(1-w_{11})(1+\bar{x}\eta)^2}{\bar{x}\bar{y}}$,

(2) a source if $\gamma > max\{-\frac{2(1+w_{11})(1+\bar{x}\eta)^2}{\bar{x}\bar{y}}, \frac{(1-w_{11})(1+\bar{x}\eta)^2}{\bar{x}\bar{y}}\}$,

(3) a saddle if $\gamma < -\frac{2(1+w_{11})(1+\bar{x}\eta)^2}{\bar{x}\bar{y}}$,

(4) non-hyperbolic, and (1.6) *experiences NS bifurcation at E_3 if $-3 < w_{11} < 1$ and $\gamma = \frac{(1-w_{11})(1+\bar{x}\eta)^2}{\bar{x}\bar{y}}$.*

Remark 2.7. *The classification of E_3 characterizes how the two populations behave near their coexistence densities. When E_3 is a sink, small deviations in the prey or predator abundances diminish over time, leading the system back to steady coexistence. If E_3 is a source or a saddle, such deviations grow, indicating that the coexistence state cannot be maintained under small ecological fluctuations. At the critical value of γ specified in condition* (4) *of Theorem 2.6, the system undergoes an NS bifurcation, through which the constant coexistence state is replaced by sustained oscillations in prey and predator densities.*

3. NS bifurcation analysis at E_3

In this section, we investigate the NS bifurcation at the interior fixed point $E_3 = (\bar{x}, \bar{y})$ of the discrete-time model (1.6) by treating γ as the primary bifurcation parameter. The NS bifurcation, also known as the discrete analogue of the Hopf bifurcation, plays a crucial role in understanding the transition from stable fixed point behavior to the emergence of closed invariant curves and quasiperiodic oscillations.

We aim to determine the conditions under which a pair of complex conjugate eigenvalues of the Jacobian matrix evaluated at E_3 cross the unit circle in the complex plane, leading to a qualitative change in the model dynamics. Specifically, we seek the critical value $\gamma = \gamma_1$ at which $|\theta_{1,2}| = 1$, with $\theta_{1,2}$ being complex conjugate eigenvalues of the Jacobian $J(E_3)$. The occurrence and nature of

the NS bifurcation depend on several nondegeneracy and transversality conditions, which ensure that the bifurcation is not degenerate and that a smooth invariant closed curve is created or destroyed as γ passes through γ_1. These conditions are established using bifurcation theory techniques presented in [37, 38].

We investigate the NS bifurcation at $E_3 = (\bar{x}, \bar{y})$ when condition (4) of Theorem 2.6 is satisfied. Applying a minor perturbation δ to γ in model (1.6), we obtain

$$\begin{cases} x_{n+1} = x_n e^{\frac{(1-x_n)(x_n-\alpha)}{x_n+\beta}-y_n}, \\ y_{n+1} = y_n e^{\frac{(\gamma+\delta)x_n}{1+\eta x_n}-\sigma}. \end{cases} \tag{3.1}$$

We shift the fixed point $E_3 = (\bar{x}, \bar{y})$ to the origin by introducing the change of variables $u_n = x_n - \bar{x}$ and $v_n = y_n - \bar{y}$. With this transformation, system (3.1) takes the following form:

$$\begin{bmatrix} u_{n+1} \\ v_{n+1} \end{bmatrix} = \begin{bmatrix} w_{11} & -\bar{x} \\ \frac{e^{\frac{\bar{x}\delta}{1+\bar{x}\eta}}\bar{y}(\delta - \frac{(-1+w_{11})(1+\bar{x}\eta)^2}{\bar{x}\bar{y}})}{(1+\bar{x}\eta)^2} & e^{\frac{\bar{x}\delta}{1+\bar{x}\eta}} \end{bmatrix} \begin{bmatrix} u_n \\ v_n \end{bmatrix} + \begin{bmatrix} \mathbb{F}_1(u_n, v_n) \\ \mathbb{F}_2(u_n, v_n) \end{bmatrix}, \tag{3.2}$$

where

$$\begin{aligned}
&\mathbb{F}_1(u_n, v_n) = a_1 u_n^2 + a_2 v_n^2 + a_3 u_n v_n + a_4 u_n^3 + a_5 v_n^3 + a_6 u_n^2 v_n + a_7 u_n v_n^2 + O((|u_n|+|v_n|)^4), \\
&\mathbb{F}_2(u_n, v_n) = b_1 u_n^2 + b_2 u_n v_n + b_3 u_n^3 + b_4 u_n^2 v_n + O((|u_n|+|v_n|)^4), \\
&a_1 = (\bar{x}^5 + \bar{x}^4(-2+4\beta) + 2\beta^2(\alpha+\beta+\alpha\beta) - 4\bar{x}^2\beta(\alpha+(4+\alpha)\beta) - 2\bar{x}^3(\alpha+(5+\alpha)\beta-2\beta^2) \\
&\quad + \bar{x}(\alpha^2 + 2\alpha(2+\alpha)\beta + (1+\alpha)(3+\alpha)\beta^2 - 6\beta^3))/(2(\bar{x}+\beta)^4), \\
&a_2 = \frac{\bar{x}}{2},\ a_3 = \frac{\bar{x}^3 - \beta^2 + \bar{x}^2(-1+2\beta) - \bar{x}(\alpha+(3+\alpha)\beta)}{(\bar{x}+\beta)^2}, \\
&a_4 = (-\bar{x}^7 + \bar{x}^6(3-6\beta) + 3\alpha^2\beta^2(1+\beta)^2 - 3\beta^4(1+2\beta) + 3\bar{x}^5(\alpha+(7+\alpha)\beta-4\beta^2) \\
&\quad - 3\bar{x}^2(\alpha^2 + 4\alpha(1+\alpha)\beta + (3+\alpha)(1+5\alpha)\beta^2 + 2(6+\alpha(6+\alpha))\beta^3 - 8\beta^4) \\
&\quad + \bar{x}^4\beta((57-8\beta)\beta + 12\alpha(1+\beta)) + \bar{x}(3\alpha^2\beta(1+\beta)^2 + \alpha^3(1+\beta)^3 - 9\alpha\beta^2(1+\beta)(1+2\beta) \\
&\quad - \beta^3(11+30\beta)) - 3\bar{x}^3((3-22\beta)\beta^2 + \alpha^2(1+\beta)^2 - 4\alpha\beta(-1+\beta^2)))/(6(\bar{x}+\beta)^6), \\
&a_5 = -\frac{\bar{x}}{6}, \\
&a_6 = (-\bar{x}^5 + \bar{x}^4(2-4\beta) - 2\beta^2(\alpha+\beta+\alpha\beta) + 4\bar{x}^2\beta(\alpha+(4+\alpha)\beta) + 2\bar{x}^3(\alpha+(5+\alpha)\beta-2\beta^2) \\
&\quad + \bar{x}(-4\alpha\beta(1+\beta) - \alpha^2(1+\beta)^2 + 3\beta^2(-1+2\beta)))/(2(\bar{x}+\beta)^4), \\
&a_7 = \frac{-\bar{x}^3 + \bar{x}^2(1-2\beta) + \beta^2 + \bar{x}(\alpha+(3+\alpha)\beta)}{2(\bar{x}+\beta)^2},\ b_1 = \frac{e^{\frac{\bar{x}\delta}{1+\bar{x}\eta}}\bar{y}(\gamma+\delta)(\gamma+\delta-2\eta(1+\bar{x}\eta))}{2(1+\bar{x}\eta)^4}, \\
&b_2 = \frac{e^{\frac{\bar{x}\delta}{1+\bar{x}\eta}}(\gamma+\delta)}{(1+\bar{x}\eta)^2},\ b_3 = \frac{e^{\frac{\bar{x}\delta}{1+\bar{x}\eta}}\bar{y}(\gamma+\delta)((\gamma+\delta)^2 - 6(\gamma+\delta)\eta - 6(-1+\bar{x}(\gamma+\delta))\eta^2 + 12\bar{x}\eta^3 + 6\bar{x}^2\eta^4)}{6(1+\bar{x}\eta)^6}, \\
&b_4 = \frac{e^{\frac{\bar{x}\delta}{1+\bar{x}\eta}}(\gamma+\delta)(\gamma+\delta-2\eta(1+\bar{x}\eta))}{2(1+\bar{x}\eta)^4}.
\end{aligned}$$

Applying condition (4) of Theorem 2.6, we find that the Jacobian matrix of system (3.2) evaluated at the origin satisfies the following characteristic equation:

$$\theta^2 - p(\delta)\theta + q(\delta) = 0, \tag{3.3}$$

where

$$p(\delta) = e^{\frac{\bar{x}\delta}{1+\bar{x}\eta}} + w_{11},\ q(\delta) = \frac{e^{\frac{\bar{x}\delta}{1+\bar{x}\eta}}(1 + \bar{x}\bar{y}\delta + \bar{x}\eta(2 + \bar{x}\eta))}{(1 + \bar{x}\eta)^2}.$$

The solutions of (3.3) are given by

$$\theta_{1,2} = \frac{p(\delta)}{2} \pm \frac{i}{2}\sqrt{4q(\delta) - p^2(\delta)}. \tag{3.4}$$

It then follows that $|\theta_{1,2}| = \sqrt{q(\delta)} = 1$. Furthermore, we compute

$$\left(\frac{d|\theta_1|}{d\delta}\right)_{\delta=0} = \left(\frac{d|\theta_2|}{d\delta}\right)_{\delta=0} = \frac{\bar{x}(1 + \bar{y} + \bar{x}\eta)}{2(1 + \bar{x}\eta)^2} > 0.$$

In addition, condition $\theta_{1,2}^i \neq 1$ must hold for $i = 1, 2, 3, 4$ when $\delta = 0$, which leads to $p(0) \neq -2, 0, 1, 2$. Employing condition (4) from Theorem 2.6, it follows that $p(0) = 1 + w_{11} \neq \pm 2$. Therefore, the remaining restrictions reduce to $p(0) \neq 0, 1$ which is equivalent to

$$w_{11} \neq -1, 0. \tag{3.5}$$

The canonical form of system (3.2) at $\delta = 0$ can be derived by implementing the linear transformation given below:

$$\begin{bmatrix} u_n \\ v_n \end{bmatrix} = \begin{bmatrix} -\bar{x} & 0 \\ \frac{1-w_{11}}{2} & \frac{-\sqrt{3 - 2w_{11} - w_{11}^2}}{2} \end{bmatrix} \begin{bmatrix} e_n \\ f_n \end{bmatrix}. \tag{3.6}$$

Substituting transformation (3.6) into system (3.2), we obtain the following form:

$$\begin{bmatrix} e_{n+1} \\ f_{n+1} \end{bmatrix} = \begin{bmatrix} \frac{1+w_{11}}{2} & \frac{-\sqrt{3 - 2w_{11} - w_{11}^2}}{2} \\ \frac{\sqrt{3 - 2w_{11} - w_{11}^2}}{2} & \frac{1+w_{11}}{2} \end{bmatrix} \begin{bmatrix} e_n \\ f_n \end{bmatrix} + \begin{bmatrix} \chi(e_n, f_n) \\ \Upsilon(e_n, f_n) \end{bmatrix}, \tag{3.7}$$

where

$$\chi(e_n, f_n) = c_1 e_n^2 + c_2 f_n^2 + c_3 e_n f_n + c_4 e_n^3 + c_5 f_n^3 + c_6 e_n^2 f_n + c_7 e_n f_n^2 + O((|e_n|+|f_n|)^4),$$
$$\Upsilon(e_n, f_n) = d_1 e_n^2 + d_2 f_n^2 + d_3 e_n f_n + d_4 e_n^3 + d_5 f_n^3 + d_6 e_n^2 f_n + d_7 e_n f_n^2 + O((|e_n|+|f_n|)^4).$$

The Appendix provides the values of the coefficients c_i and d_j. To identify the direction of the NS bifurcation, the first Lyapunov exponent is calculated as follows:

$$L = \left(\left[-Re\left(\frac{(1 - 2\theta_1)\theta_2^2}{1 - \theta_1}\tau_{20}\tau_{11}\right) - \frac{1}{2}|\tau_{11}|^2 - |\tau_{02}|^2 + Re(\theta_2\tau_{21})\right]\right)_{\delta=0}, \tag{3.8}$$

where the values of τ_{20}, τ_{11}, τ_{02}, and τ_{21} are derived from the Taylor expansions of the functions $\chi(e_n, f_n)$ and $\Upsilon(e_n, f_n)$ in the canonical form (3.7). They are computed using the following standard formulas from bifurcation theory [37, 38]:

$$\tau_{20} = \frac{1}{8}\left[\chi_{e_ne_n} - \chi_{f_nf_n} + 2\Upsilon_{e_nf_n} + i(\Upsilon_{e_ne_n} - \Upsilon_{f_nf_n} - 2\chi_{e_nf_n})\right],$$
$$\tau_{11} = \frac{1}{4}\left[\chi_{e_ne_n} + \chi_{f_nf_n} + i(\Upsilon_{e_ne_n} + \Upsilon_{f_nf_n})\right],$$
$$\tau_{02} = \frac{1}{8}\left[\chi_{e_ne_n} - \chi_{f_nf_n} - 2\Upsilon_{e_nf_n} + i(\Upsilon_{e_ne_n} - \Upsilon_{f_nf_n} + 2\chi_{e_nf_n})\right],$$
$$\tau_{21} = \frac{1}{16}\left[\chi_{e_ne_ne_n} + \chi_{e_nf_nf_n} + \Upsilon_{e_ne_nf_n} + \Upsilon_{f_nf_nf_n} + i(\Upsilon_{e_ne_ne_n} + \Upsilon_{e_nf_nf_n} - \chi_{e_ne_nf_n} - \chi_{f_nf_nf_n})\right],$$

where the subscripts denote partial derivatives evaluated at $(e_n, f_n) = (0, 0)$. Based on the above analysis, we obtain the following result:

Theorem 3.1. *Suppose that condition* (4) *of Theorem 2.6 holds. If the first Lyapunov coefficient L given in* (3.8) *is non-zero and condition* (3.5) *is true, then model* (1.6) *undergoes an NS bifurcation at the fixed point E_3, as the bifurcation parameter γ varies in a neighborhood of the critical value $\gamma_1 = \frac{(1-w_{11})(1+\bar{x}\eta)^2}{\bar{x}\bar{y}}$. Moreover, if $L < 0$ (respectively, $L > 0$), the NS bifurcation is supercritical (respectively, subcritical), and a unique closed invariant curve bifurcates from E_3, which is attracting (respectively, repelling).*

Remark 3.2. *The occurrence of a NS bifurcation signifies that steady coexistence becomes unstable and gives rise to persistent oscillations in both species. From an ecological perspective, this represents predator-prey cycles driven by nonlinear density dependence and the combined influence of two Allee effects. The amplitude and frequency of these oscillations depend on how strongly low-density effects restrict prey growth. Thus, the NS bifurcation identifies critical ecological thresholds separating stable coexistence from cyclic population behavior.*

4. Numerical simulations and bifurcation analysis

In this section, we present numerical simulations to illustrate the stability and bifurcation behavior of the model. By systematically varying key parameters, we analyze their impact on the model's equilibrium stability and the emergence of complex dynamical patterns. Our primary focus is on detecting NS bifurcations, where a stable equilibrium loses stability and gives rise to quasi-periodic oscillations. This transition is crucial in ecological modeling, as it signifies persistent cyclic interactions between predator and prey populations. We use MATHEMATICA for computations and MATLAB for plotting the graphs.

The numerical simulations provide insight into how ecological interactions and environmental factors shape predator-prey dynamics. By systematically varying key parameters, we observe transitions from stable coexistence to oscillatory behavior, which reflects real-world ecological scenarios, where population cycles emerge due to changes in resource availability, predation pressure, or species interactions. The transformed parameters $(\alpha, \beta, \gamma, \eta, \sigma)$ encapsulate these ecological effects in a more compact mathematical framework while retaining their biological significance.

Numerical simulations show how changes in prey growth parameters and predator efficiency modify long-term population dynamics. If the Allee thresholds are strong, then prey populations may fall to

levels from which recovery is difficult, thereby leading indirectly to predator population reduction. On the other hand, if predation pressure or conversion efficiency is high, then increases in the predator populations may destabilize the recoveries of their prey and generate oscillations. These results demonstrate the ecological relevance of the double Allee effect by illustrating how multiple low-density limitations can amplify or suppress predator-prey cycles.

4.1. Effect of γ on stability and bifurcation

We examine the effect of the bifurcation parameter γ while keeping other parameters fixed at $\alpha = -0.66$, $\beta = 0.93$, $\eta = 0.88$, and $\sigma = 0.85$. For these parameter values, the model undergoes an NS bifurcation at $\gamma \approx 2.810381$. The corresponding positive fixed point is $E_3 \approx (0.412145, 0.469596)$. The eigenvalues of the Jacobian matrix evaluated at E_3 are $\theta_{1,2} = 0.853541 \pm 0.521026i$, which satisfy condition $|\theta_{1,2}| = 1$. This verifies that (1.6) experiences NS bifurcation at $\gamma \approx 2.810381$. Moreover, we obtain

$$\tau_{20} = -0.0476695 - 0.0521211i, \quad \tau_{11} = 0.018306 + 0.0799617i,$$
$$\tau_{02} = 0.20171 + 0.170237i, \quad \tau_{21} = 0.0150405 - 0.0087488i.$$

Thus, it is obtained that $L = -0.0515658 < 0$, which shows that NS bifurcation is supercritical.

To further illustrate this transition, we present bifurcation diagrams for x_n and y_n over the range $\gamma \in [2.70, 3.20]$, as shown in Figures 2(a) and 2(b). The initial conditions are set as $x_0 = 0.40$ and $y_0 = 0.45$. The diagrams indicate that for $\gamma < 2.810381$, E_3 is stable. However, as γ increases beyond the bifurcation threshold $\gamma \approx 2.810381$, the stability of E_3 is lost due to NS bifurcation. This bifurcation signifies a transition from a stable fixed point to a stable limit cycle, where the model exhibits quasi-periodic oscillations. Figure 2(c) presents the corresponding graph of the maximum Lyapunov exponent (MLE).

Figure 3 illustrates the phase portraits of the model for different values of γ. These phase portraits provide insight into the dynamical transition of the model. For lower values of γ, such as $2.76, 2.78$ and 2.80 (Figures 3(a) and 3(c)), trajectories spiral toward equilibrium point E_3, indicating local stability. As γ increases toward the bifurcation threshold ($\gamma \approx 2.810381$), the phase portraits change significantly. At $\gamma = 2.82$ (Figure 3(d)), an emerging closed invariant curve can be observed, suggesting the onset of quasi-periodic nature. For $\gamma > 2.810381$ (Figures 3(e)–3(i)), the fixed point E_3 loses stability, and trajectories evolve into a stable closed orbit. Figure 3(j) shows that the radius of invariant is increasing as we increase the value of γ. This closed curve represents persistent oscillations, characteristic of an NS bifurcation. This transition highlights the impact of bifurcation parameter γ on the model's dynamics, showing how small changes in environmental or interaction factors can lead to significant qualitative shifts in predator-prey population behavior.

Although we present the numerical simulations in this section for specific parameter sets, the qualitative behaviors reported therein, such as the instability of E_3 via an NS bifurcation, closed invariant curves, and transitions between stable and oscillatory regions, are independent of these choices. In our additional computations for larger regions of the biologically feasible parameter space, we find that the NS bifurcation occurs so long as condition $\gamma = \frac{(1-w_{11})(1+\bar{x}\eta)^2}{\bar{x}\bar{y}}$ is met and the nondegeneracy conditions of Theorem 3.1 are satisfied. The simulations below must therefore be understood as representative examples of general dynamical structures exhibited by the model, rather than as isolated behaviors restricted to any single parameter choice.

One crucial finding is the impact of γ, which represents the predator's efficiency in converting prey biomass into its own growth. As γ increases, meaning the predator becomes more effective at utilizing prey for reproduction, the model transitions from a stable equilibrium to a state of persistent oscillations due to an NS bifurcation. Ecologically, this corresponds to a scenario where improved predator efficiency leads to a destabilizing feedback loop: A high conversion rate initially benefits the predator, but as prey declines due to excessive predation, the predator population also experiences fluctuations. This pattern is commonly observed in nature when predator populations lag behind prey abundance, resulting in periodic predator-prey cycles, such as those seen in lynx-hare or wolf-moose models.

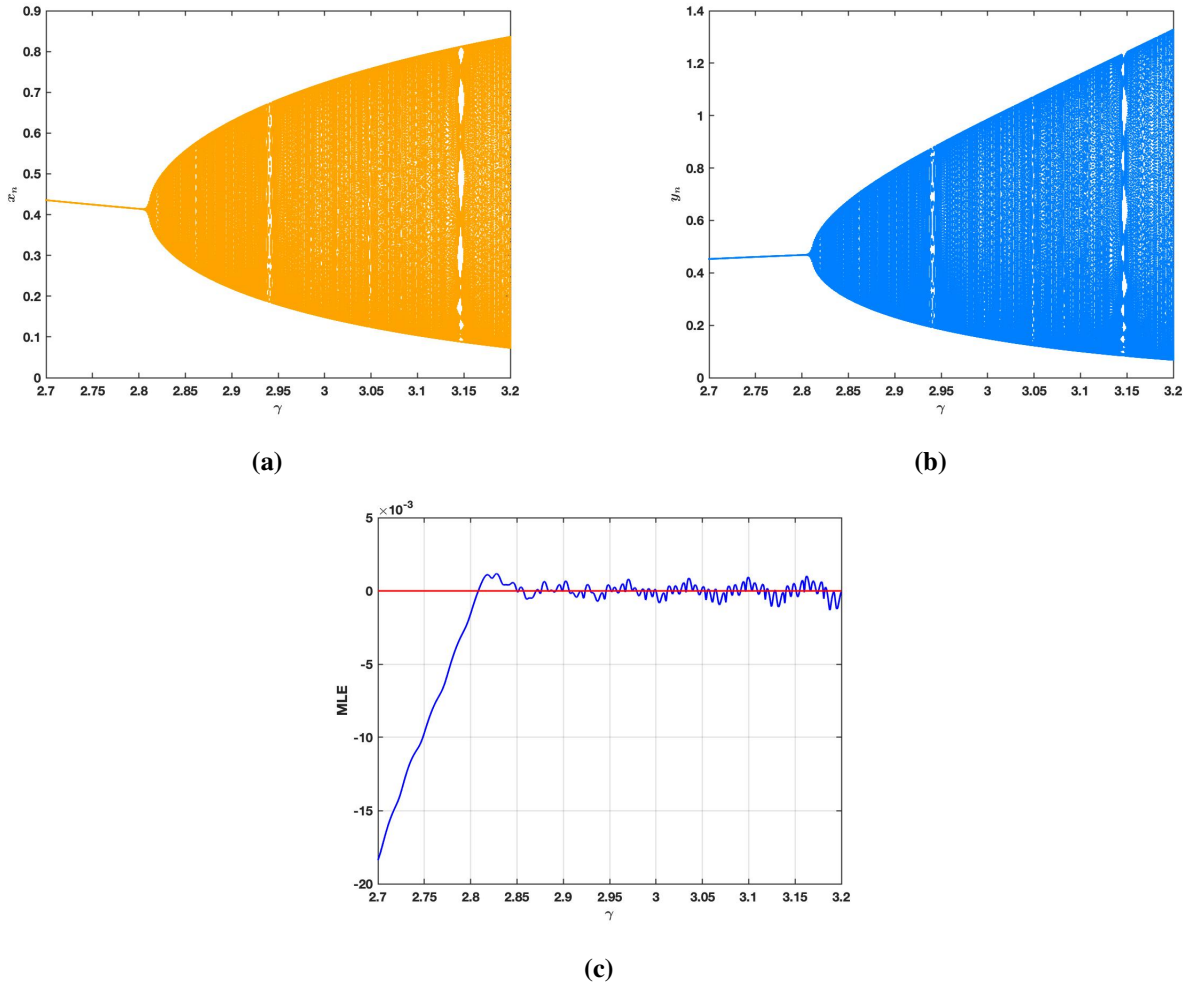

Figure 2. Bifurcation diagrams and MLE graph of model (1.6) as γ varies. Fixed parameter values are $\alpha = -0.66$, $\beta = 0.93$, $\eta = 0.88$, and $\sigma = 0.85$ and initial conditions are $x_0 = 0.40$ and $y_0 = 0.45$.

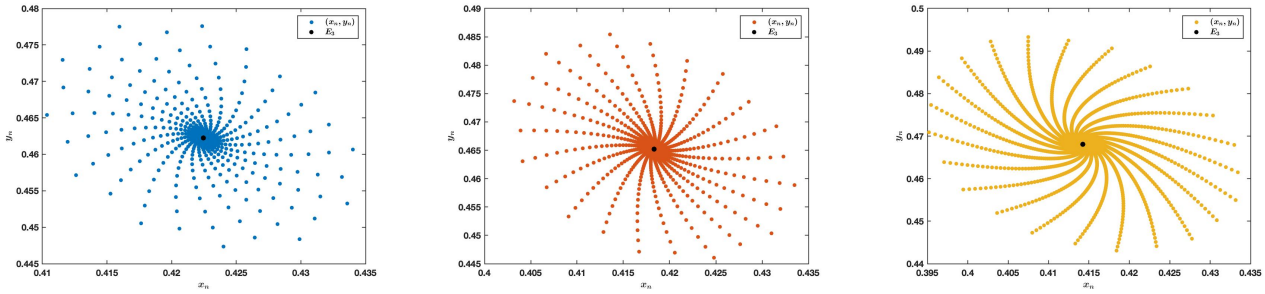

(a) $\gamma = 2.76$ **(b)** $\gamma = 2.78$ **(c)** $\gamma = 2.80$

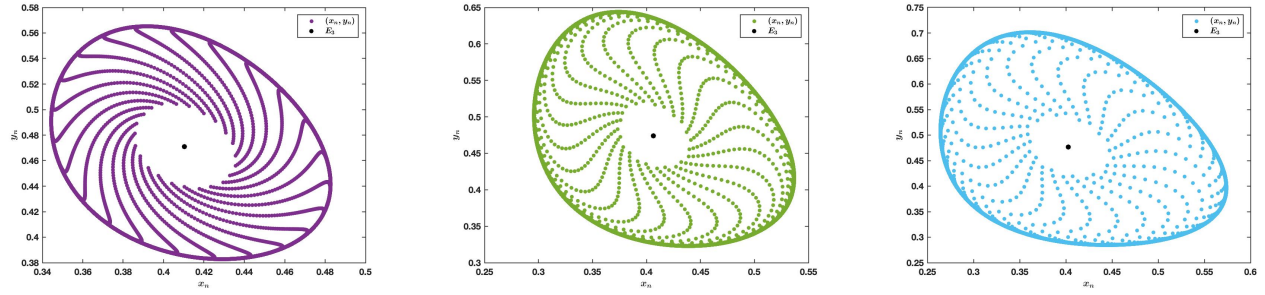

(d) $\gamma = 2.82$ **(e)** $\gamma = 2.84$ **(f)** $\gamma = 2.86$

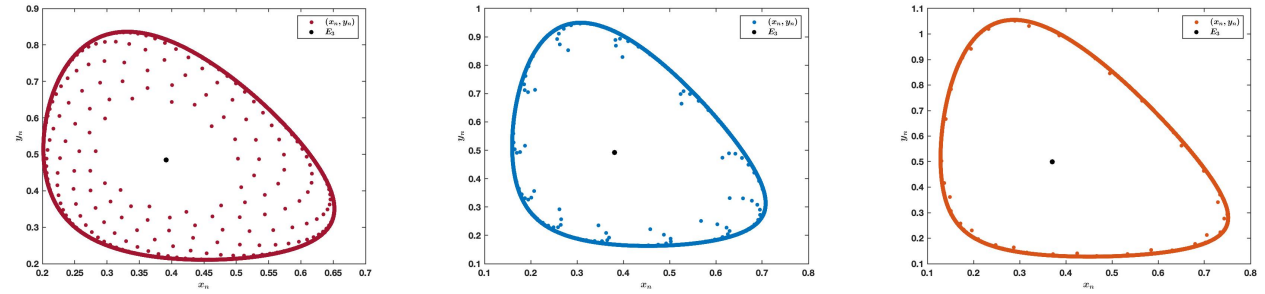

(g) $\gamma = 2.92$ **(h)** $\gamma = 2.98$ **(i)** $\gamma = 3.04$

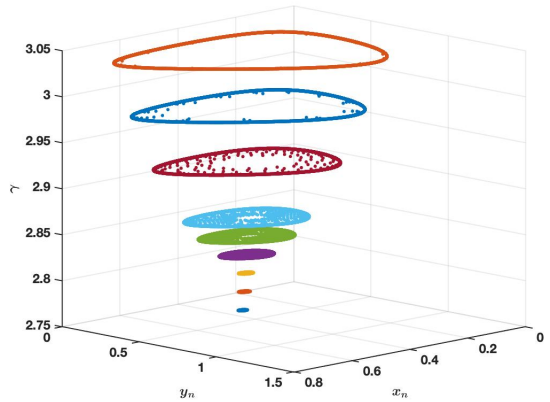

(j)

Figure 3. Phase portraits of (1.6) by varying γ and fixing $\alpha = -0.66$, $\beta = 0.93$, $\eta = 0.88$, $\sigma = 0.85$, $x_0 = 0.40$, and $y_0 = 0.45$.

4.2. *Effect of α, β, η, and σ on stability and bifurcation*

The dynamics of model (1.6) are also influenced by other parameters. To further explore the bifurcation behavior, we fix $\beta = 0.45$, $\gamma = 1.8$, $\eta = 0.11$, and $\sigma = 0.45$ and vary α within the interval $[-0.75, -0.55]$. The bifurcation analysis reveals that NS bifurcation occurs at $\alpha \approx -0.688157$, where the positive fixed point $E_3 \approx (0.257069, 0.993166)$ loses stability. The bifurcation diagrams in Figure 4, generated with initial conditions $x_0 = 0.25$ and $y_0 = 0.95$, illustrate this transition. As α approaches the critical value, the fixed point destabilizes due to NS bifurcation. This indicates the emergence of quasi-periodic oscillations in the predator-prey interactions, leading to cyclic population dynamics instead of convergence to a steady equilibrium. Figure 4(c) depicts the corresponding MLE graph.

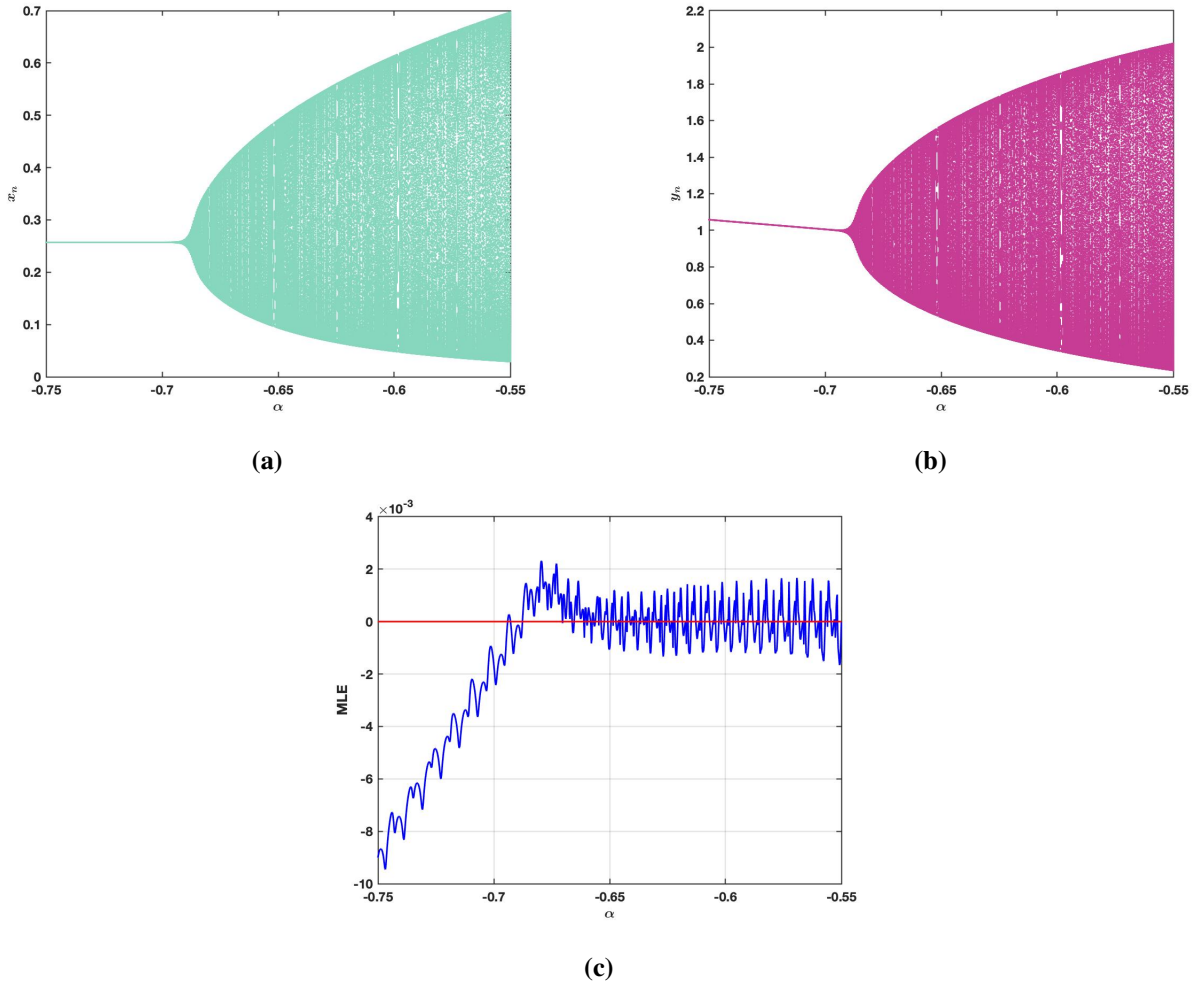

Figure 4. Bifurcation diagrams and the corresponding MLE plot of (1.6) with respect to the variation of α. The fixed parameter values are $\beta = 0.45$, $\gamma = 1.8$, $\eta = 0.11$, and $\sigma = 0.45$, while the initial conditions are $x_0 = 0.25$ and $y_0 = 0.95$.

α, associated with the Allee effect threshold, plays a crucial role in determining whether a prey population can persist. When α is too high (indicating a strong Allee effect), the model becomes more vulnerable to extinction, as prey populations struggle to recover when numbers fall below a critical

level. However, as α decreases, indicating a weaker Allee effect, the model stabilizes, enabling more sustainable coexistence. This is particularly relevant in conservation biology, where species subjected to strong Allee effects, such as certain fish or insect populations, face higher extinction risks if their numbers drop too low.

To further explore the impact of parameter variations on the model's dynamics, we now fix $\alpha = -0.43$, $\gamma = 1.17$, $\eta = 0.22$, and $\sigma = 0.12$ and allow β to vary over the interval $[0.35, 0.55]$. When β is relatively small, the model stabilizes at the positive fixed point $E_3 \approx (0.104932, 0.895338)$. However, as β increases, stability is lost at the critical threshold $\beta \approx 0.429839$, triggering an NS bifurcation. The bifurcation diagrams in Figure 5, plotted with initial conditions $x_0 = 0.15$ and $y_0 = 0.85$, illustrate this transition from stability to quasi-periodic oscillations. The related MLE plot is given in Figure 5(c).

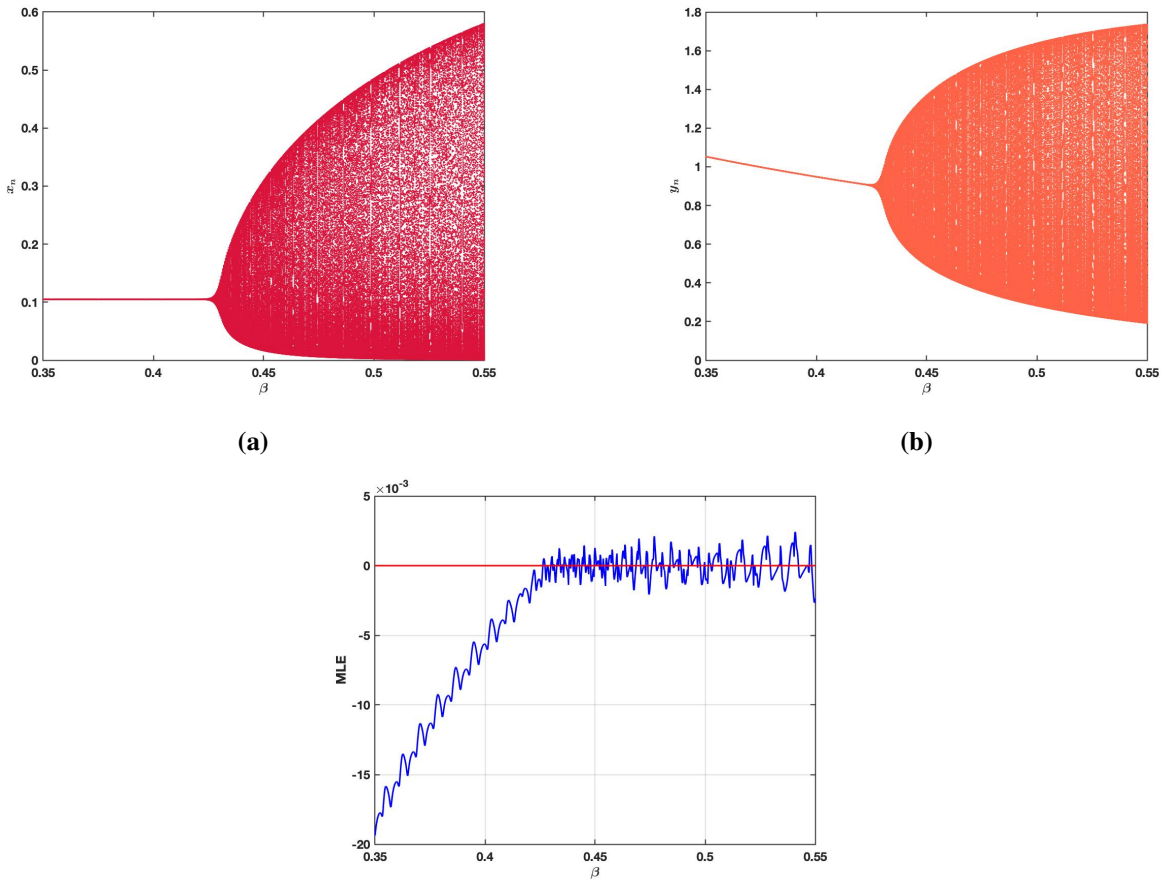

Figure 5. Bifurcation diagrams and MLE plot of model (1.6) changing β and fixing $\alpha = -0.43$, $\gamma = 1.17$, $\eta = 0.22$, and $\sigma = 0.12$, and initial values are $x_0 = 0.15$ and $y_0 = 0.85$.

β, which represents the second Allee effect component, influences model stability by modifying the reproductive success of the prey population. As β increases, the threshold for sustainable population growth becomes higher, making the model more prone to oscillations or population collapses. This suggests that environmental factors limiting fertility, such as habitat fragmentation or pollution, can lead to increased population instability, emphasizing the importance of maintaining suitable

reproductive conditions for species conservation.

To investigate the impact of η on the model's dynamics, we set $\alpha = 0.54, \beta = 0.4, \gamma = 1.7$, and $\sigma = 0.77$ and vary η within the range $[0.88, 0.92]$. The bifurcation analysis reveals that for smaller values of η, the model exhibits NS bifurcation. However, as η increases beyond the critical value $\eta \approx 0.897359$, the model stabilizes at the positive fixed point $E_3 \approx (0.763106, 0.045441)$. The bifurcation diagrams are given in Figure 6 using initial conditions $x_0 = 0.80$ and $y_0 = 0.05$. The MLE plot is depicted in Figure 6(c).

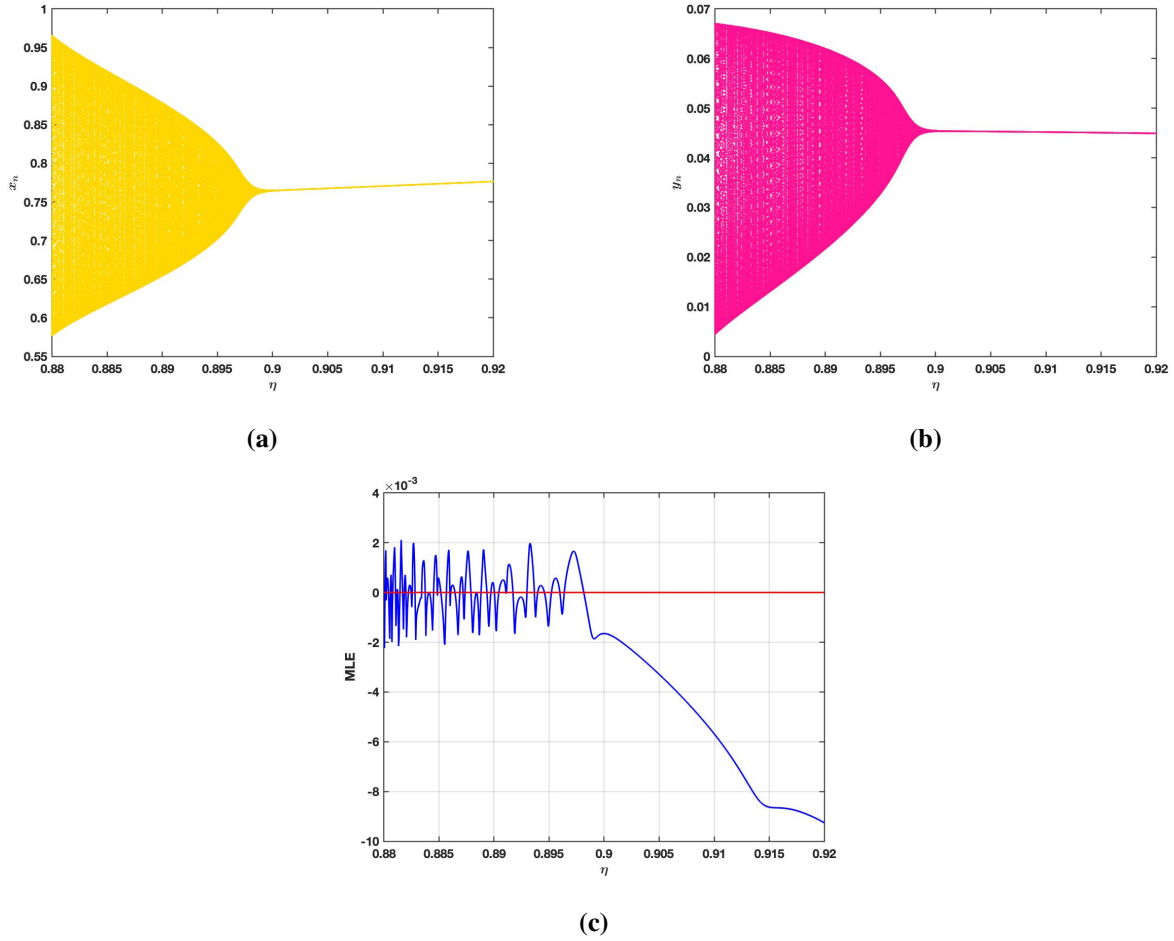

Figure 6. Bifurcation diagrams and MLE graph of model (1.6) as η varies. Fixed parameter values are $\alpha = 0.54$, $\beta = 0.4$, $\gamma = 1.7$, and $\sigma = 0.77$, and initial values are $x_0 = 0.80$ and $y_0 = 0.05$.

η controls the saturation effect in the predator's response to prey density. For lower values of η, the model exhibits NS bifurcation, leading to instability and oscillatory predator-prey cycles. This suggests that when the predator's response to prey is less saturated, small disturbances can amplify, resulting in persistent fluctuations in population sizes. However, as η increases, the model stabilizes, leading to a stable positive fixed point where both species coexist in equilibrium. Ecologically, this implies that a higher saturation effect in the predator's functional response helps regulate prey consumption in a way that promotes long-term stability. Such stabilization can be attributed to a more controlled predation

rate that prevents excessive depletion of prey, a phenomenon commonly observed in ecosystems where predators adjust their foraging strategies in response to prey abundance.

Next, we analyze the effect of σ on the model's dynamics by fixing $\alpha = 0.67$, $\beta = 1.57$, $\gamma = 0.93$, and $\eta = 0.88$, while varying σ within the range $[0.4455, 0.4555]$. The bifurcation analysis reveals that for smaller values of σ, the model exhibits quasi-periodic oscillations, indicating the occurrence of NS bifurcation at $\sigma \approx 0.447182$. As σ increases beyond this threshold, the model stabilizes at the positive fixed point $E_3 \approx (0.833549, 0.011326)$. This transition is depicted in Figure 7, where bifurcation diagrams are plotted using the initial conditions $x_0 = 0.85$ and $y_0 = 0.01$. The corresponding MLE graph is given in Figure 7(c).

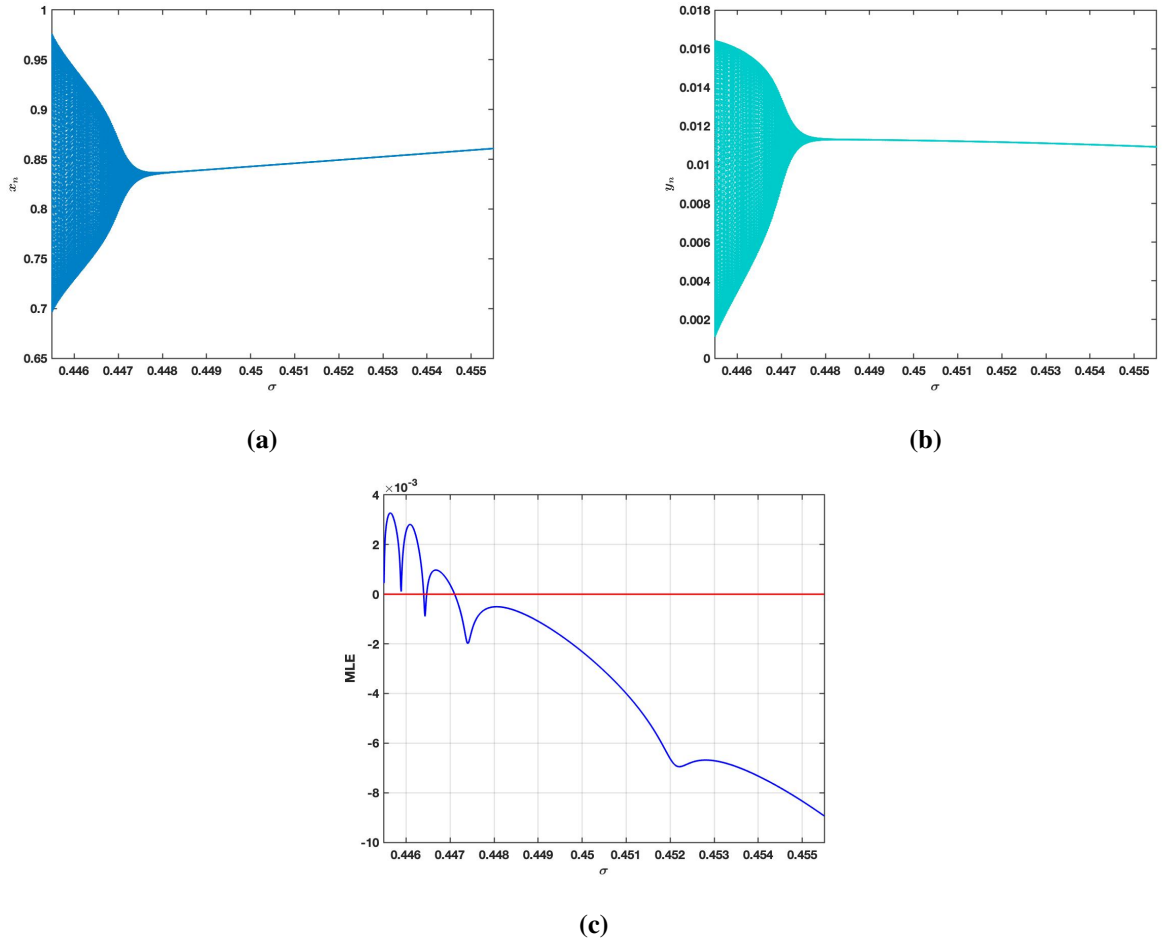

Figure 7. Bifurcation diagrams and MLE plot of model (1.6) changing σ, and fixing $\alpha = 0.67$, $\beta = 1.57$, $\gamma = 0.93$, and $\eta = 0.88$ and initial conditions are $x_0 = 0.85$ and $y_0 = 0.01$.

σ, which is the predator mortality rate relative to the prey growth rate, has a stabilizing effect when increased. Higher σ values imply that predators face greater mortality pressure, preventing unchecked predator growth and thereby reducing oscillatory fluctuations in the model. However, when σ is too low, predators persist even when prey numbers decline, leading to prolonged periods of instability. This reflects ecological scenarios where predator overpopulation, in the absence of sufficient natural mortality, can drive prey to dangerously low levels, disrupting ecosystem balance.

4.3. Comparative dynamics with and without the Allee effect

In this section, we demonstrate the significant impact of the Allee effect on the long-term behavior of a discrete predator-prey model. In particular, we show that incorporating the Allee effect can substantially slow the convergence to the model's interior fixed point and alter the model's qualitative dynamics.

We begin by considering model (1.6) under the influence of a double Allee effect, with the following parameter values:

$$\alpha = -0.66,\ \beta = 0.93,\ \eta = 0.88,\ \sigma = 0.85,$$

and initial conditions $x_0 = 0.40$ and $y_0 = 0.45$. For two different values of γ : 2.80 and 2.81, we analyze the behavior of the model.

Under these settings, we obtain $E_3 \approx (0.41423, 0.468113)$ for $\gamma = 2.80$ and $E_3 \approx (0.412221, 0.469542)$ for $\gamma = 2.81$.

To assess the role of the Allee effect, we compare the above with a simplified version of the model in which the Allee effect is removed. The resulting discrete-time model is

$$\begin{cases} x_{n+1} = x_n e^{1-x_n-y_n}, \\ y_{n+1} = y_n e^{\frac{\gamma x_n}{1+\eta x_n}-\sigma}. \end{cases} \tag{4.1}$$

Using the same parametric and initial values, the positive fixed point of the model (4.1) (without the Allee effect) is calculated as $(0.41423, 0.58577)$ for $\gamma = 2.80$, and $(0.412221, 0.587779)$ for $\gamma = 2.81$. A direct comparison of these fixed points reveals that, while the prey equilibrium value remains unchanged, the predator equilibrium is significantly lower in the presence of the Allee effect. This indicates that the Allee effect reduces the predator's ability to maintain a higher population level, likely due to decreased prey availability or efficiency at low prey densities.

Figure 8 presents the time series plots and phase portraits for models (1.6) (blue) and (4.1) (red). From the time series plots given in Figures 8(a)–8(e), we observe that the model incorporating the Allee effect converges to the fixed point more slowly, suggesting a delay in population recovery and stabilization. Biologically, this aligns with the interpretation of the Allee effect: At low population sizes, individuals face challenges in reproduction and survival, which slows growth and prolongs instability.

Furthermore, the model without the Allee effect (4.1) shows stable convergence to its interior fixed point (see Figures 8(j)–8(l)), indicating local asymptotic stability. In contrast, the model with the Allee effect (1.6) exhibits oscillatory behavior near the fixed point and eventually undergoes an NS bifurcation (see Figures 8(g)–8(i)). This bifurcation gives rise to quasiperiodic dynamics, where population levels oscillate indefinitely without settling at a fixed point.

Ecologically, these findings emphasize the critical role of the Allee effect in shaping population dynamics. The introduction of a double Allee effect creates a threshold-dependent dynamic, resulting in a significant deceleration of population growth at low densities, perhaps preventing the model from achieving a stable equilibrium. The presence of an NS bifurcation indicates the possibility of sustained oscillations in population densities, which may develop into intricate or chaotic patterns when the model operates near key parameter thresholds.

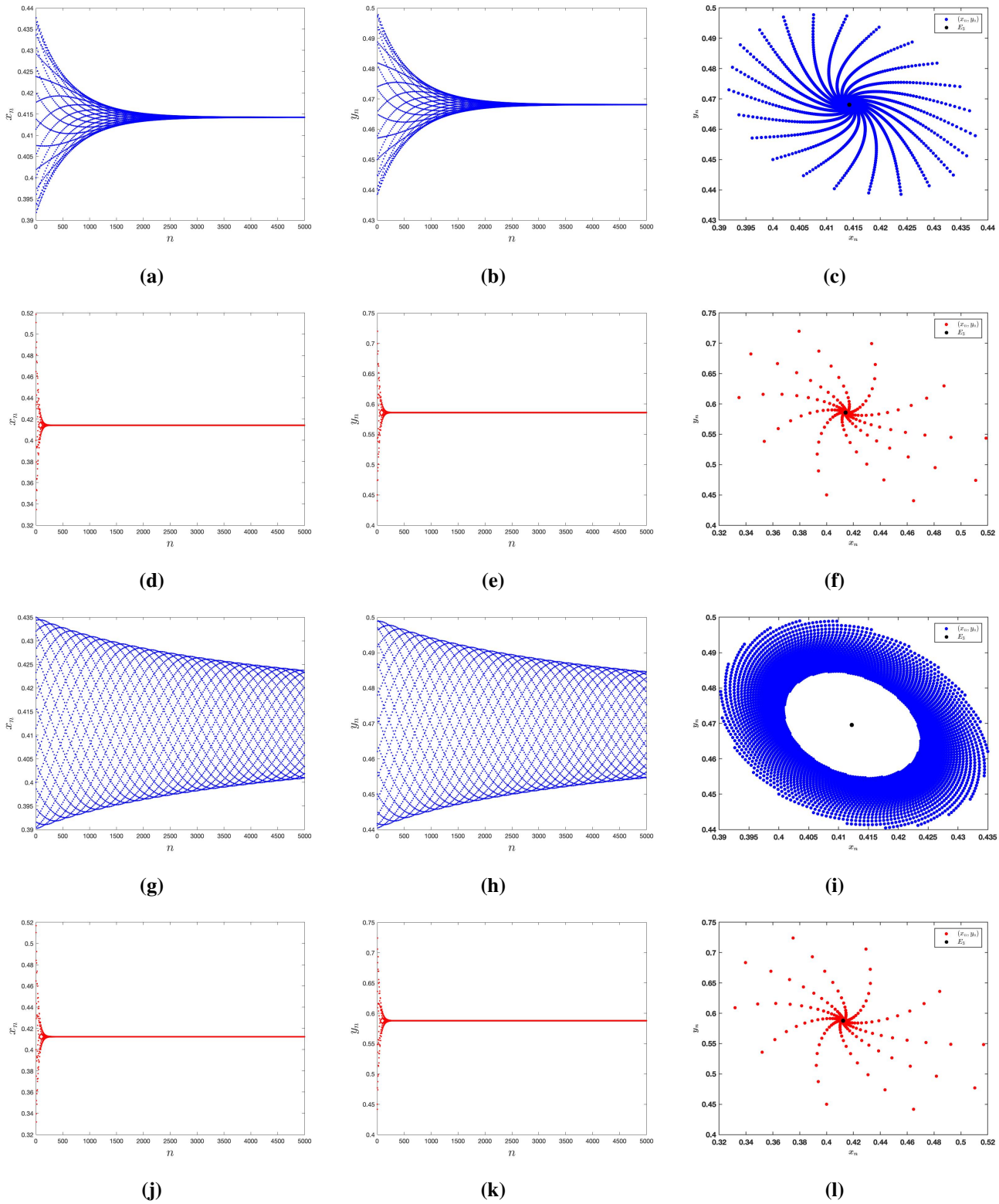

Figure 8. Time series plots and phase portraits of model (1.6) (blue) and model (4.1) (red) for the parameter values $\alpha = -0.66$, $\beta = 0.93$, $\eta = 0.88$, and $\sigma = 0.85$ and initial conditions $x_0 = 0.40$, and $y_0 = 0.45$. Figures 8(a)–8(f) correspond to $\gamma = 0.80$, while Figures 8(g)–8(l) correspond to $\gamma = 2.81$.

The comparison demonstrates that the inclusion of the Allee effect modifies the locations of equilibrium points and significantly influences the model's stability and asymptotic behavior. These results are crucial for conservation and population management, particularly in settings where low population densities may increase extinction risks owing to Allee effects.

5. Conclusions

In this study, we analyze the dynamics of a discrete-time predator-prey model, including a double Allee effect on the prey population. We examine the influence of the Allee effect on predator-prey interactions via the analysis of fixed points, stability, and bifurcation analysis. The model has four equilibrium points: Extinction (E_0), two prey-only equilibria (E_1 and E_2), and a coexistence equilibrium (E_3). The stability study demonstrates that the Allee effect substantially affects the model's long-term results. Our bifurcation analysis indicates that if certain parameters fluctuate, the positive equilibrium may become unstable via an NS bifurcation, resulting in quasi-periodic oscillations that resemble natural population cycles.

The mathematical categorization of coexistence equilibrium reveals under what conditions a predator-prey model can support stable coexistence in the long term and when extinction or persistent cycles may prevail. The NS threshold defines the transition from steady coexistence to persistent oscillations, signaling nonlinear prey growth-driven recurrent population cycles with low-density effects. These findings illustrate how specific ecological mechanisms impact long-term consequences and may assist in the development of management practices that avoid collapse for systems prone to strict low-density constraints.

We found that higher Allee effects disrupt the dynamics, increasing the risk of extinction or long-term oscillations. On the other hand, higher predator mortality and a more pronounced saturation in the predator's functional response help stabilize the model. A comparison of models with and without the Allee effect reveals that adding Allee dynamics slows the system's convergence to equilibrium and may cause instability. These findings have important implications for conservation efforts, especially for species with small populations that are at danger of extinction owing to high Allee thresholds. The results emphasize the significance of careful ecosystem management in areas where such impacts exist.

Biologically, the results of this study show how the interaction of two low-density mechanisms can drastically modify the predator-prey dynamics. If prey density is small enough, either the threshold-type Allee effect or the density-dependent performance factor limits recovery and increases the risk of extinction. Furthermore, these limitations alter the relative balance between prey growth and predation to produce shifts between stable coexistence and oscillatory dynamics. The analytical and numerical results thus provide insight into how real ecosystems may respond to collective reproductive limitations, predation pressure, and environmental restrictions.

Although we develop a valuable understanding of the dynamics of predator-prey models with multiple Allee effect, limitations should not be overlooked. The dynamics observed are contingent on our choice of the piecewise constant argument method for discretization. While this method effectively preserves non-negative solutions and key dynamical features, alternative discretization techniques (e.g., the Mickens-type non-standard finite difference scheme) may yield quantitatively different bifurcation thresholds or stability regions. A comparative study of different discretization methods, as well as a

detailed analytical comparison with the corresponding continuous-time model, are valuable directions for future research.

Author contributions

Asifa Tassaddiq: Investigation, Methodology, Validation, Writing–original draft; Rizwan Ahmed: Conceptualization, Methodology, Software, Writing–original draft; Jawad Khan: Investigation, Project administration, Software, Validation, Writing–review & editing; Youngmoon Lee: Formal analysis, Funding acquisition, Methodology, Resources, Supervision, Writing–review & editing. All authors have read and agreed to the published version of the manuscript.

Use of Generative-AI tools declaration

The authors declare they have not used Artificial Intelligence (AI) tools in the creation of this article.

Acknowledgments

This work was supported in part by Institute of Information and Communications Technology Planning and Evaluation (IITP) (grant IITP-2025-RS-2020-II201741 and RS-2024-00423071) and National Research Foundation of Korea (NRF) BK21 grant Education/Research/Industry-Centric physical AI: ERICA all funded by the Korea government (MSIT, MOE). The authors extend the appreciation to the Deanship of Postgraduate Studies and Scientific Research at Majmaah University for funding this research work through the project number (ER-2025-2116).

Conflict of interest

The authors have no conflicts of interest to disclose.

References

1. A. J. Lotka, Elements of physical biology, *Nature*, **116** (1925), 461. https://doi.org/10.1038/116461b0
2. V. Volterra, Fluctuations in the abundance of a species considered mathematically, *Nature*, **118** (1926), 558–560. http://dx.doi.org/10.1038/118558a0
3. K. Sarkar, S. Khajanchi, P. C. Mali, J. J. Nieto, Rich dynamics of a predator-prey system with different kinds of functional responses, *Complexity*, **2020** (2020), 4285294. https://doi.org/10.1155/2020/4285294
4. M. Alsubhi, R. Ahmed, I. Alraddadi, F. Alsharif, M. Imran, Stability and bifurcation analysis of a discrete-time plant-herbivore model with harvesting effect, *AIMS Math.*, **9** (2024), 20014–20042. https://doi.org/10.3934/math.2024976
5. M. S. Shabbir, Q. Din, Understanding cannibalism dynamics in predator-prey interactions: bifurcations and chaos control strategies, *Qual. Theory Dyn. Syst.*, **23** (2024), 53. https://doi.org/10.1007/s12346-023-00908-7

6. X. Y. Wang, L. Zanette, X. F. Zou, Modelling the fear effect in predator-prey interactions, *J. Math. Biol.*, **73** (2016), 1179–1204. https://doi.org/10.1007/s00285-016-0989-1
7. F. Y. Zhu, R. Z. Yang, Bifurcation in a modified Leslie-Gower model with nonlocal competition and fear effect, *Discrete Contin. Dyn. Syst. S*, **30** (2025), 2865–2893. https://doi.org/10.3934/dcdsb.2024195
8. I. M. Alsulami, R. Ahmed, F. Ashraf, Exploring complex dynamics in a Ricker type predator-prey model with prey refuge, *Chaos*, **35** (2025), 023107. https://doi.org/10.1063/5.0232030
9. R. Ahmed, S. Akhtar, U. Farooq, S. Ali, Stability, bifurcation, and chaos control of predator-prey system with additive Allee effect, *Commun. Math. Biol. Neurosci.*, **2023** (2023), 1–25. https://doi.org/10.28919/cmbn/7824
10. P. A. Naik, R. Ahmed, A. Faizan, Theoretical and numerical bifurcation analysis of a discrete predator-prey system of Ricker type with weak Allee effect, *Qual. Theory Dyn. Syst.*, **23** (2024), 260. https://doi.org/10.1007/s12346-024-01124-7
11. A. A. Khabyah, R. Ahmed, M. S. Akram, S. Akhtar, Stability, bifurcation, and chaos control in a discrete predator-prey model with strong Allee effect, *AIMS Math.*, **8** (2023), 8060–8081. https://doi.org/10.3934/math.2023408
12. W. C. Allee, *Animal aggregations, a study in general sociology*, The University of Chicago Press, 1931. https://doi.org/10.5962/bhl.title.7313
13. Z. C. Shang, Y. H. Qiao, Bifurcation analysis in a predator-prey model with strong Allee effect on prey and density-dependent mortality of predator, *Math. Methods Appl. Sci.*, **47** (2024), 3021–3040. https://doi.org/10.1002/mma.9793
14. R. Kumbhakar, S. Pal, N. Pal, P. K. Tiwari, Bistability and tristability in a predator-prey model with strong Allee effect in prey, *J. Biol. Syst.*, **31** (2023), 215–243. https://doi.org/10.1142/s0218339023500110
15. L. M. Zhang, T. Wang, Qualitative properties, bifurcations and chaos of a discrete predator-prey system with weak Allee effect on the predator, *Chaos Solitons Fract.*, **175** (2023), 113995. https://doi.org/10.1016/j.chaos.2023.113995
16. Y. R. Dong, H. Liu, Y. M. Wei, Q. B. Zhang, G. Ma, Stability and Hopf bifurcation analysis of a predator-prey model with weak Allee effect delay and competition delay, *Mathematics*, **12** (2024), 2853. https://doi.org/10.3390/math12182853
17. Y. N. Zeng, P. Yu, Complex dynamics of predator-prey systems with Allee effect, *Int. J. Bifur. Chaos*, **32** (2022), 2250203. https://doi.org/10.1142/s0218127422502030
18. Y. Z. Liu, Z. Y. Zhang, Z. Li, The impact of Allee effect on a Leslie-Gower predator-prey model with hunting cooperation, *Qual. Theory Dyn. Syst.*, **23** (2024), 88. https://doi.org/10.1007/s12346-023-00940-7
19. F. D. Chen, Z. Li, Q. Pan, Q. Zhu, Bifurcations in a Leslie-Gower predator-prey model with strong Allee effects and constant prey refuges, *Chaos Solitons Fract.*, **192** (2025), 115994. https://doi.org/10.1016/j.chaos.2025.115994
20. Y. D. Ma, M. Zhao, Y. F. Du, Impact of the strong Allee effect in a predator-prey model, *AIMS Math.*, **7** (2022), 16296–16314. https://doi.org/10.3934/math.2022890

21. B. Tiwari, S. N. Raw, Dynamics of Leslie-Gower model with double Allee effect on prey and mutual interference among predators, *Nonlinear Dyn.*, **103** (2021), 1229–1257. https://doi.org/10.1007/s11071-020-06095-3

22. F. T. Wang, R. Z. Yang, X. Zhang, Turing patterns in a predator-prey model with double Allee effect, *Math. Comput. Simul.*, **220** (2024), 170–191. https://doi.org/10.1016/j.matcom.2024.01.015

23. J. F. Jiao, C. Chen, Bogdanov-Takens bifurcation analysis of a delayed predator-prey system with double Allee effect, *Nonlinear Dyn.*, **104** (2021), 1697–1707. https://doi.org/10.1007/s11071-021-06338-x

24. G. Mandal, L. N. Guin, S. Chakravarty, R. J. Han, Dynamic complexities in a predator-prey model with prey refuge influenced by double Allee effects, *Math. Comput. Simul.*, **227** (2025), 527–552. https://doi.org/10.1016/j.matcom.2024.08.015

25. P. J. Pal, T. Saha, Qualitative analysis of a predator-prey system with double Allee effect in prey, *Chaos Solitons Fract.*, **73** (2015), 36–63. https://doi.org/10.1016/j.chaos.2014.12.007

26. F. T. Wang, R. Z. Yang, Dynamics of a delayed reaction-diffusion predator-prey model with nonlocal competition and double Allee effect in prey, *Int. J. Biomath.*, **18** (2025), 2350097. https://doi.org/10.1142/s1793524523500973

27. C. Mondal, R. Mondal, D. Kesh, D. Mukherjee, Dynamics of predator-prey system with the consequences of double Allee effect in prey population, *J. Biol. Phys.*, **51** (2025), 5. https://doi.org/10.1007/s10867-025-09670-0

28. P. A. Naik, Z. Eskandari, Z. Avazzadeh, J. Zu, Multiple bifurcations of a discrete-time prey-predator model with mixed functional response, *Int. J. Bifur. Chaos*, **32** (2022), 2250050. https://doi.org/10.1142/s021812742250050x

29. A. Suleman, A. Q. Khan, R. Ahmed, Bifurcation analysis of a discrete Leslie-Gower predator-prey model with slow-fast effect on predator, *Math. Methods Appl. Sci.*, **47** (2024), 8561–8580. https://doi.org/10.1002/mma.10032

30. P. A. Naik, M. Amer, R. Ahmed, S. Qureshi, Z. X. Huang, Stability and bifurcation analysis of a discrete predator-prey system of Ricker type with refuge effect, *Math. Biosci. Eng.*, **21** (2024), 4554–4586. https://doi.org/10.3934/mbe.2024201

31. R. Ahmed, N. Tahir, N. A. Shah, An analysis of the stability and bifurcation of a discrete-time predator-prey model with the slow-fast effect on the predator, *Chaos*, **34** (2024), 033127. https://doi.org/10.1063/5.0185809

32. P. Baydemir, H. Merdan, E. Karaoglu, G. Sucu, Complex dynamics of a discrete-time prey-predator system with Leslie type: stability, bifurcation analyses and chaos, *Int. J. Bifur. Chaos*, **30** (2020), 2050149. https://doi.org/10.1142/s0218127420501497

33. R. Ahmed, A. Q. Khan, M. Amer, A. Faizan, I. Ahmed, Complex dynamics of a discretized predator-prey system with prey refuge using a piecewise constant argument method, *Int. J. Bifur. Chaos*, **34** (2024), 2450120. https://doi.org/10.1142/s0218127424501207

34. P. A. Naik, Y. Javaid, R. Ahmed, Z. Eskandari, A. H. Ganie, Stability and bifurcation analysis of a population dynamic model with Allee effect via piecewise constant argument method, *J. Appl. Math. Comput.*, **70** (2024), 4189–4218. https://doi.org/10.1007/s12190-024-02119-y

35. S. F. Aldosary, R. Ahmed, Stability and bifurcation analysis of a discrete Leslie predator-prey system via piecewise constant argument method, *AIMS Math.*, **9** (2024), 4684–4706. https://doi.org/10.3934/math.2024226

36. A. C. Luo, *Regularity and complexity in dynamical systems*, New York: Springer, 2012. http://dx.doi.org/10.1007/978-1-4614-1524-4

37. J. Guckenheimer, P. Holmes, *Nonlinear oscillations, dynamical systems, and bifurcations of vector fields*, New York: Springer, 1983. http://dx.doi.org/10.1007/978-1-4612-1140-2

38. S. Wiggins, *Introduction to applied nonlinear dynamical systems and chaos*, New York: Springer, 1990. http://dx.doi.org/10.1007/978-1-4757-4067-7

Appendix

List of coefficients associated with the nonlinear terms of system (3.7):

$$
\begin{aligned}
c_1 &= \frac{1}{8(\bar{x}+\beta)^4}\Big(- 4\bar{x}^6 - (-5+w_{11})(-1+w_{11})\beta^4 - 4\bar{x}^5(-3+w_{11}+4\beta)\\
&\quad + 4\bar{x}\beta^2(-((8+(-7+w_{11})w_{11})\beta) + (-3+w_{11})\alpha(1+\beta)) - \bar{x}^4(5+w_{11}^2 - 8\alpha(1+\beta)\\
&\quad + 8\beta(-7+2\beta) + 2w_{11}(-3+8\beta)) + 2\bar{x}^2(4(-3+w_{11})\alpha\beta(1+\beta) - 2\alpha^2(1+\beta)^2\\
&\quad + \beta^2(-25+w_{11}(22-3w_{11}-4\beta)+16\beta)) + 4\bar{x}^3(\alpha(1+\beta)(-1+w_{11}+4\beta)\\
&\quad - \beta(6-21\beta+w_{11}(-7+w_{11}+5\beta)))\Big),\\
c_2 &= \frac{(-1+w_{11})(3+w_{11})}{8},\\
c_3 &= -\frac{\sqrt{3-2w_{11}-w_{11}^2}}{4(\bar{x}+\beta)^2}\Big(2\bar{x}^3 + (-3+w_{11})\beta^2 + \bar{x}^2(-3+w_{11}+4\beta) - 2\bar{x}(\alpha+(4-w_{11}+\alpha)\beta)\Big),\\
c_4 &= \frac{1}{6}\Big(- \frac{1}{8}(-1+w_{11})^3 - \frac{3(-1+w_{11})^2(\bar{x}^3-\beta^2+\bar{x}^2(-1+2\beta)-\bar{x}(\alpha+(3+\alpha)\beta))}{4(\bar{x}+\beta)^2}\\
&\quad - \frac{1}{2(\bar{x}+\beta)^4}3(-1+w_{11})\bar{x}(\bar{x}^5+\bar{x}^4(-2+4\beta)+2\beta^2(\alpha+\beta+\alpha\beta) - 4\bar{x}^2\beta(\alpha+(4+\alpha)\beta)\\
&\quad - 2\bar{x}^3(\alpha+(5+\alpha)\beta-2\beta^2)+\bar{x}(\alpha^2+2\alpha(2+\alpha)\beta+(1+\alpha)(3+\alpha)\beta^2-6\beta^3))\\
&\quad + \frac{1}{(\bar{x}+\beta)^6}\bar{x}^2(-\bar{x}^7+\bar{x}^6(3-6\beta)+3\alpha^2\beta^2(1+\beta)^2-3\beta^4(1+2\beta)+3\bar{x}^5(\alpha+(7+\alpha)\beta-4\beta^2)\\
&\quad - 3\bar{x}^2(\alpha^2+4\alpha(1+\alpha)\beta+(3+\alpha)(1+5\alpha)\beta^2+2(6+\alpha(6+\alpha))\beta^3-8\beta^4)\\
&\quad + \bar{x}^4\beta((57-8\beta)\beta+12\alpha(1+\beta))+\bar{x}(3\alpha^2\beta(1+\beta)^2+\alpha^3(1+\beta)^3-9\alpha\beta^2(1+\beta)(1+2\beta)\\
&\quad - \beta^3(11+30\beta)) - 3\bar{x}^3((3-22\beta)\beta^2+\alpha^2(1+\beta)^2-4\alpha\beta(-1+\beta^2)))\Big),\\
c_5 &= -\frac{(3-2w_{11}-w_{11}^2)^{3/2}}{48},\\
c_6 &= -\frac{\sqrt{3-2w_{11}-w_{11}^2}}{16(\bar{x}+\beta)^4}\Big(4\bar{x}^6+(-5+w_{11})(-1+w_{11})\beta^4+4\bar{x}^5(-3+w_{11}+4\beta)\\
&\quad + 4\bar{x}\beta^2((8+(-7+w_{11})w_{11})\beta-(-3+w_{11})\alpha(1+\beta))
\end{aligned}
$$

$$
\begin{aligned}
&+ \bar{x}^4(5 + w_{11}^2 - 8\alpha(1+\beta) + 8\beta(-7+2\beta) + 2w_{11}(-3+8\beta))\\
&+ 2\bar{x}^2(-4(-3+w_{11})\alpha\beta(1+\beta) + 2\alpha^2(1+\beta)^2 + \beta^2(25 - 22w_{11} + 3w_{11}^2 + 4(-4+w_{11})\beta))\\
&- 4\bar{x}^3(\alpha(1+\beta)(-1+w_{11}+4\beta) - \beta(6 - 21\beta + w_{11}(-7+w_{11}+5\beta)))\Big),\\
c_7 &= \frac{(-1+w_{11})(3+w_{11})}{16(\bar{x}+\beta)^2}\Big(2\bar{x}^3 + (-3+w_{11})\beta^2 + \bar{x}^2(-3+w_{11}+4\beta) - 2\bar{x}(\alpha + (4 - w_{11} + \alpha)\beta)\Big),\\
d_1 &= \frac{-1+w_{11}}{8\sqrt{3 - 2w_{11} - w_{11}^2}}\Big(\frac{8e^{-\frac{(-1+w_{11})(1+\bar{x}\eta)}{\bar{y}} - \sigma}(-1+w_{11})}{\bar{y}} + \frac{1}{(\bar{x}+\beta)^4}(4\bar{x}^6 + (5 - 6w_{11} + w_{11}^2)\beta^4\\
&+ 4\bar{x}^5(-3+w_{11}+4\beta) - 4\bar{x}\beta^2(-((8 - 7w_{11} + w_{11}^2)\beta) + (-3+w_{11})\alpha(1+\beta))\\
&+ \bar{x}^4(5 + w_{11}^2 - 56\beta + 16\beta^2 - 8\alpha(1+\beta) + 2w_{11}(-3+8\beta))\\
&+ \bar{x}^2(-8(-3+w_{11})\alpha\beta(1+\beta) + 4\alpha^2(1+\beta)^2 + 2\beta^2(25 + 3w_{11}^2 - 16\beta + w_{11}(-22+4\beta)))\\
&- 4\bar{x}^3(\alpha(1+\beta)(-1+w_{11}+4\beta) - \beta(6 + w_{11}^2 - 21\beta + w_{11}(-7+5\beta))))\\
&- \frac{8e^{-\frac{(-1+w_{11})(1+\bar{x}\eta)}{\bar{y}} - \sigma}(-1 + w_{11} + w_{11}\bar{x}\eta + \bar{x}(-1+2\bar{y})\eta)}{\bar{y} + \bar{x}\bar{y}\eta}\Big),\\
d_2 &= \frac{(-1+w_{11})\sqrt{3 - 2w_{11} - w_{11}^2}}{8},\\
d_3 &= \frac{(-1+w_{11})e^{-\frac{(-1+w_{11})(1+\bar{x}\eta)}{\bar{y}} - \sigma}}{4\bar{y}(\bar{x}+\beta)^2}\Big(4(\bar{x}+\beta)^2 + e^{\frac{(-1+w_{11})(1+\bar{x}\eta)}{\bar{y}} + \sigma}\bar{y}(2\bar{x}^3 + (-3+w_{11})\beta^2\\
&+ \bar{x}^2(-3+w_{11}+4\beta) - 2\bar{x}(\alpha + 4\beta - w_{11}\beta + \alpha\beta))\Big),\\
d_4 &= \frac{(-1+w_{11})}{48\sqrt{3 - 2w_{11} - w_{11}^2}}\Big(((-1+w_{11})^3 + \frac{6(-1+w_{11})^2(\bar{x}^3 - \beta^2 + \bar{x}^2(-1+2\beta) - \bar{x}(\alpha + 3\beta + \alpha\beta))}{(\bar{x}+\beta)^2}\\
&+ \frac{1}{(\bar{x}+\beta)^4}12(-1+w_{11})\bar{x}(\bar{x}^5 + \bar{x}^4(-2+4\beta) + 2\beta^2(\alpha+\beta+\alpha\beta) - 4\bar{x}^2\beta(\alpha+4\beta+\alpha\beta)\\
&- 2\bar{x}^3((5-2\beta)\beta + \alpha(1+\beta)) + \bar{x}(3(1-2\beta)\beta^2 + 4\alpha\beta(1+\beta) + \alpha^2(1+\beta)^2))\\
&- \frac{1}{(\bar{x}+\beta)^6}8\bar{x}^2(-\bar{x}^7 + \bar{x}^6(3-6\beta) + 3\alpha^2\beta^2(1+\beta)^2 - 3\beta^4(1+2\beta) + 3\bar{x}^5(\alpha + (7+\alpha)\beta - 4\beta^2)\\
&- 3\bar{x}^2(\alpha^2 + 4\alpha(1+\alpha)\beta + (3+\alpha)(1+5\alpha)\beta^2 + 2(6+\alpha(6+\alpha))\beta^3 - 8\beta^4)\\
&+ \bar{x}^4\beta((57-8\beta)\beta + 12\alpha(1+\beta)) + \bar{x}(3\alpha^2\beta(1+\beta)^2 + \alpha^3(1+\beta)^3 - 9\alpha\beta^2(1+\beta)(1+2\beta)\\
&- \beta^3(11+30\beta)) - 3\bar{x}^3((3-22\beta)\beta^2 + \alpha^2(1+\beta)^2 - 4\alpha\beta(-1+\beta^2))))\\
&+ \frac{24e^{-\frac{(-1+w_{11})(1+\bar{x}\eta)}{\bar{y}} - \sigma}(-1+w_{11})(-1 + w_{11} + w_{11}\bar{x}\eta + \bar{x}(-1+2\bar{y})\eta)}{\bar{y}^2(1+\bar{x}\eta)}\\
&- \frac{1}{(\bar{y} + \bar{x}\bar{y}\eta)^2}16e^{-\frac{(-1+w_{11})(1+\bar{x}\eta)}{\bar{y}} - \sigma}(1 + \bar{x}(2-6\bar{y})\eta + \bar{x}^2(1 - 6\bar{y} + 6\bar{y}^2)\eta^2 + (w_{11} + w_{11}\bar{x}\eta)^2\\
&+ 2w_{11}(1+\bar{x}\eta)(-1 + \bar{x}(-1+3\bar{y})\eta))\Big),\\
d_5 &= -\frac{(-1+w_{11})^2(3+w_{11})}{48},
\end{aligned}
$$

$$
\begin{aligned}
d_6 = \frac{(-1+w_{11})}{16}\Big(&\frac{1}{(\bar{x}+\beta)^4}(4\bar{x}^6 + (5-6w_{11}+w_{11}^2)\beta^4 + 4\bar{x}^5(-3+w_{11}+4\beta)\\
&- 4\bar{x}\beta^2(-((8-7w_{11}+w_{11}^2)\beta) + (-3+w_{11})\alpha(1+\beta))\\
&+ \bar{x}^4(5+w_{11}^2-56\beta+16\beta^2-8\alpha(1+\beta)+2w_{11}(-3+8\beta))\\
&+ \bar{x}^2(-8(-3+w_{11})\alpha\beta(1+\beta)+4\alpha^2(1+\beta)^2+2\beta^2(25+3w_{11}^2-16\beta+w_{11}(-22+4\beta)))\\
&- 4\bar{x}^3(\alpha(1+\beta)(-1+w_{11}+4\beta)-\beta(6+w_{11}^2-21\beta+w_{11}(-7+5\beta))))\\
&+ \frac{8e^{-\frac{(-1+w_{11})(1+\bar{x}\eta)}{\bar{y}}-\sigma}(-1+w_{11}+w_{11}\bar{x}\eta+\bar{x}(-1+2\bar{y})\eta)}{\bar{y}^2(1+\bar{x}\eta)}\Big),\\
d_7 = -\Big(&((-1+w_{11})^2(3+w_{11})(2\bar{x}^3+(-3+w_{11})\beta^2+\bar{x}^2(-3+w_{11}+4\beta)\\
&- 2\bar{x}(\alpha+4\beta-w_{11}\beta+\alpha\beta))\Big)\Big/\Big(16\sqrt{3-2w_{11}-w_{11}^2}(\bar{x}+\beta)^2\Big).
\end{aligned}
$$

AIMS Press